

Controls on Near-Surface Soil Moisture Dynamics within a Tidal Marsh-Forested Upland
Coastal Environment

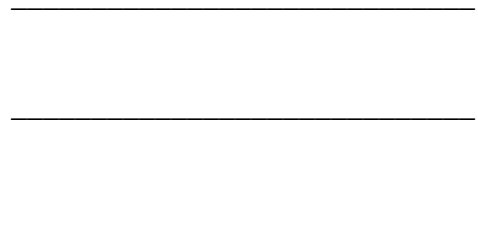
Scott Dusterhoff
Baltimore, MD

B.S., University of Maryland, 1996

A Thesis presented to the Graduate Faculty
of the University of Virginia in Candidacy for the Degree of
Masters of Science

Department of Environmental Sciences

University of Virginia
August 2001



LIST OF FIGURES

- 2.1 Schematic diagram of water table dynamics in a coastal environments
- 2.2 Study site location within Phillips Creek marsh on the Delmarva Peninsula
- 2.3 Longitudinal profile of the study transect
- 2.4 Site variables for Phillips Creek marsh during the summer of 1999
- 2.5 Inundation frequency on the study transect for the summer of 1999
- 2.6 Pore water salinity within the top 30 cm of soil along the study transect
- 2.7 Soil organic matter content within the top 30 cm of soil for the study transect
- 2.8 Average low-tide water table elevation along the study transect
- 2.9 Time series of soil moisture within the top 30 cm of soil for the study transect
- 2.10 Time-averaged soil moisture and soil moisture variability along the study transect
- 2.11 Time series of tidally-induced water table fluctuations at well 70
- 2.12 Relationship of water table rise at well 70 and high tide elevation
- 2.13 Tidal importance on soil moisture dynamics for varying soil texture and elevation

- 3.1 Schematic diagram of root water uptake dynamics
- 3.2 Root fraction with depth function used for modeling root water uptake
- 3.3 Root efficiency reduction function used for modeling root water uptake
- 3.4 Measured and modeled soil moisture at the study site for the summer of 1999
- 3.5 Modeled soil moisture in the organic litter layer and underlying loam
- 3.6 Measured potential evapotranspiration and modeled root water uptake
- 3.7 Modeled time series of root water uptake at the study site

- 3.8 Modeled root water uptake with and without the presence of an organic litter layer
 - 3.9 Root fraction with depth for different vegetation types
 - 3.10 Percent of total roots in the top 10 cm for different root density distributions
 - 3.11 Modeled saturation time and total root water uptake
 - 3.12 Representative plots of modeled saturation time and total root water uptake
-
- A.1 Calibration curve for the CS615 soil moisture probes used at the study site

LIST OF TABLES

- 2.1 Soil hydraulic properties for the study site
- 3.1 Soil hydraulic properties for the soil textures considered in modeling soil moisture

Chapter 1: General Introduction

Soil moisture in watershed systems is important in the control of vegetation dynamics, land-atmosphere interactions, and transport of materials. Available soil water is an important factor in determining the occurrence of vegetation species as well as a significant control on the exchange of water vapor from vegetation and the ground surface to the atmosphere. In particular, soil saturation dynamics govern overland flow generation, thereby controlling the rate of delivery of both sediment and solutes from higher elevations to lower elevations and subsequent watershed drainage network. Topography has been acknowledged as an important factor in controlling spatial and temporal dynamics of soil saturation at the catchment scale. Prediction of areas of saturation within catchments has been widely accomplished by using a topographic index model (TOPMODEL) developed by Beven and Kirkby (1979), which determines saturated areas based primarily on topographic controls. In the coastal environment considered in this study where a tidal salt marsh is adjacent to an upland forest, the topographic gradient is low. The gentle terrain along the transition from marsh to upland coupled with a diurnal tidal signal in this environment suggests mechanisms other than topography being the dominant control on surface saturation dynamics. Site variables such as soil and vegetation type, along with the tidal forcing component, can be considered important factors in driving soil moisture dynamics in tidal regions where topographic control on soil saturation is diminished.

The overall goal of this research was to determine how soil texture, vegetation rooting dynamics, and tidal forcing control the distribution of soil moisture dynamics within a

tidal marsh-forested upland environment. The main questions addressed within the context of this research are: 1) How do soil texture and elevation mediate tidal forcing affects on soil moisture dynamics on varying time scales?, and 2) What role does the coupling of soil texture and root density distribution with depth have on controlling surface saturation dynamics? The first question is addressed in Chapter 2 by analysis of field measurements of soil moisture and water table elevation along the transition from marsh to upland. The control of tidal forcing on soil saturation is then examined by determining the magnitude of tidal importance on water table fluctuations and subsequent soil moisture as a function of soil texture and elevation. The second question is addressed in Chapter 3 by first using a model developed for this study to predict soil moisture dynamics with and without soil layering characteristics of upland forest ecosystems. The model is then used to predict surface saturation dynamics for soil textures with varying root density distributions. The ultimate goal of this thesis is to provide new and pertinent insight into the understanding and prediction of saturation dynamics along low lying, tidal marsh-upland forest ecosystems.

Chapter 2: Controls on Near-Surface Soil Moisture Dynamics Along a Marsh-Upland Transition Zone

2.1 INTRODUCTION

Soil moisture dynamics in coastal ecosystems are important in controlling the surface and subsurface delivery of materials along elevations gradients. Within coastal environments where upland ecosystems border tidal salt marshes, soil moisture dynamics control the delivery of both sediment and solutes from upland sources to low-lying marsh ecosystems and tidal waters. Along the transition from marsh to upland, soil moisture is significantly affected by tidal influences. Tidal forcing can control soil moisture dynamics within this environment by either direct tidal inundation or by tidally induced water table fluctuation (Figure 2.1). The affect of tidal inundation on soil moisture is constrained, on average, to the lower elevations closer to the tidal signal while tidally induced water table fluctuations can extend farther into upland regions. Factors that contribute to the effect of tidal forcing water table fluctuations and soil moisture dynamics are soil texture and distance from the tidal signal, which is comparable to elevation. Therefore, a feedback mechanism exists where soil moisture controls the delivery of materials from the higher elevation sources to tidal environments and tidal forcing controls the soil moisture dynamics within the higher elevations by forcing water table fluctuations. Determining the control of soil texture and elevation in mediating tidal effects on soil moisture along a marsh-upland transition zone can be crucial in understanding both the spatial and temporal dynamics of soil moisture, which can lead to a better understanding of solute and sediment delivery within this coastal ecosystem.

The transition zone between the marsh and the upland is characterized by vegetation zonation that is associated with tidal inundation (Hmieleski, 1994). As ground elevation increases from the marsh to the upland, salt-tolerant high marsh vegetation gives way to forested plant species. The transition zone between marsh and forest ecosystems contains a combination of marsh and terrestrial vegetation due to frequency of tidal inundation and an associated salinity gradient in this region. Tidal inundation within the transition occurs with enough frequency that marsh vegetation can thrive yet not so frequent that forest vegetation can not survive. Over time, the position of the transition zone will migrate landward due to an increase in mean tidal elevation (and a corresponding increase in frequency of tidal inundation) caused by a rise in mean sea level (Brinson *et al.*, 1995). Areas of research along the transition zone include soil evolution (Gardner, 1992), vegetation and pore water characterization (Hmieleski, 1994), transitional ecotone development (Brinson *et al.*, 1995), and groundwater dynamics (Harvey, 1986; Harvey *et al.*, 1988; Harvey and Odum, 1990; Hmieleski, 1994). The dependence of biological and chemical processes on hydrologic processes in this transitional environment is beginning to be realized by researchers. Consequently, hydrologic interactions that exist between tidal salt marshes and adjacent uplands are gaining significant attention.

Within tidal salt marsh environments, soil moisture is significantly affected by soil physical properties mediating the infiltration and evaporation of tidal water (Hemond and Fifield, 1982; Hemond, *et. al.*, 1984; Knott, *et. al.*, 1987; Nuttle and Hemond, 1988). Surface sediments in tidal marshes are characterized by high silt and clay contents, resulting in low average infiltration rates. Infiltration rates of tidal salt marsh sediments are in the range of 1.5 mm/day (Harvey and Nuttle, 1995; Nuttle and Harvey, 1995) to 5

mm/day (Hemond *et al.*, 1984; Harvey *et al.*, 1987). The degree of infiltration into marsh sediments is augmented by macroporosity associated with bioturbation (Mendelsohn and Seneca, 1980; Howes *et al.*, 1981; Bertness, 1985; Ridd, 1996; Hughes *et al.*, 1998). The presence of macropores in marsh soils has been shown to increase infiltration by 1 to 2 orders of magnitude (Hughes *et al.*, 1998). Estimates of macroporosity in tidal salt marshes include 5% of total pore volume (Harvey and Nuttle, 1995) and 1% of total marsh surface area (Hughes *et al.*, 1998). Harvey and Nuttle (1995) showed that the vertical fluxes of water and solutes are segregated by pore size, with the infiltration occurring in sediment macropores and upward flow and evaporation occurring from the matrix pores. The sediment stores a much greater quantity of water in the matrix pores than in the macropores (Harvey, 1993), and therefore, the saturated pore space that is exposed to the atmosphere on the marsh surface when the marsh surface is exposed is predominantly matrix pores. The evaporative demand, then, is satisfied by a flux of water from the matrix pores (Harvey and Nuttle, 1995).

Seasonal water table dynamics along the marsh-upland transition vary spatially and temporally as a function of tidal and precipitation inputs. In a study conducted in a freshwater tidal marsh on the Eastern Shore of Virginia, Harvey (1986) found an average annual hydraulic gradient from an upland hillslope towards the marsh indicating groundwater input into the marsh environment from the upland. Groundwater input from the upland into the marsh for the Harvey (1986) study was irregular on a seasonal time scale. The water table elevations in the marsh were lowest during the late summer months (low precipitation input) and highest in the late fall. During summer months with little precipitation input, spring tides caused the marsh to act as a source of water for the

high marsh-upland transition and upland. When precipitation input into the sediment increased, the water table elevation rose and the upland served as a source for subsurface water to the marsh (Harvey, 1986). Hmieleski (1994) found that the highest mean monthly water table values for an entire year were within the transition zone and the lowest mean monthly water table values were in the upland fringe within a tidal salt marsh on the Virginia coast. The largest variability in water table values between the high marsh, marsh-upland transition, and the upland fringe recorded by Hmieleski (1994) was in the summer months due to low precipitation inputs. Water table elevations in the high marsh had little seasonal variation, the transition zone had a higher degree of seasonal variation, and the upland fringe showed the largest degree of seasonal variability in water table elevation (Hmieleski, 1994).

On a tidal time scale, coastal environments exhibit water table fluctuations because of tidal forcing (Lanyon *et al.*, 1982, Nielson, 1990, Li *et al.*, 2000a, Li *et al.*, 2000b). The magnitude of the water table response to tidal forcing is a function of tidal range, aquifer hydraulic properties, and distance from the tidal signal (Li *et al.*, 1997). Within coastal environments dominated by sandy soils, the extent of inland propagation of the tidal signal on water table fluctuation has been shown to extend hundreds of meters inland (Lanyon *et al.*, 1982, Li *et al.*, 2000a). Through an analytical analysis of tidal forcing on groundwater fluctuation, Li *et al.* (2000a) showed that in a homogeneous sandy environment, the semi-diurnal tidal signal on water table fluctuation is attenuated within 100 m from the shoreline while the spring-neap tide signal is evident on water table elevation 200 m inland. Lag time between high tide and maximum water table elevation in these high permeability near-shore regions where semi-diurnal tides have an effect on

water table fluctuation can be on the order 2 hours at a distance of 20 m from the intersection between mean sea level and beach slope (Nielsen, 1990).

High silt and clay contents within salt marsh sediments result in a diminished impact of tidal forcing on water table fluctuations. In marsh environments adjacent to tidal creeks, previous studies have shown that the range in distance from the tidal creek bank where the water table is affected by semi-diurnal tides is on the order of tens of meters from the creek bank due to fine sediment size distributions (Nuttle and Hemond, 1988; Hughes *et al.*, 1998). Nuttle and Hemond (1988) found that within a tidal salt marsh with a average saturated hydraulic conductivity of 0.0342 cm/min and an average tidal range in the adjacent creek of 2 m, tidal forcing on water table fluctuation was negligible 10 m from the creek bank. Groundwater fluctuations by tidal forcing within a tidal environment with a tidal range of 0.5 m and with a low conductivity mud layer overlying a silty sand layer (saturated hydraulic conductivity of 1 cm/min) extended to a distance of 20 m from the tidal creek bank with no time lag between high tide and peak water table elevation (Hughes *et al.*, 1998).

Understanding the spatial and temporal soil moisture dynamics along the marsh-upland transition zone is essential in understanding the interaction between terrestrial and marine environments. Soil moisture dynamics within this environment control the run-off generation and delivery of sediment and solutes from upland regions to low-lying salt marshes and adjacent marine systems. The controls on salt marsh hydrology have been well established and groundwater dynamics across a high marsh-upland transition have been documented on both tidal and seasonal time scales. Previous research in this environment, however, has not addressed the degree of soil saturation across the

transition from marsh to upland on a seasonal time scale or the controls on average soil moisture for a range of tidal cycles. Furthermore, tidal-scale water table fluctuations along the marsh-upland transition are important in determining soil moisture dynamics and require further consideration. Although there have been efforts to predict the extent of water table fluctuations within coastal environments (i.e., Baird, *et al.*, 1998; Li *et al.*, 2000a), the role of tidally induced water table fluctuations on controlling soil moisture along a marsh-upland transition has not been explored. A better understanding of the controls on water table rise affecting soil moisture can be important in predicting soil saturation and run-off generation dynamics within coastal systems.

This project was designed to examine the interaction between elevation and soil texture on the control of root zone soil moisture along the gradient from marsh to upland on varying time scales. Specifically, the goals of this project were to: 1) Examine the control of elevation on the spatial distribution of near-surface soil moisture dynamics on a seasonal time scale, and 2) Determine how elevation and texture can control the relative importance of tidal forcing on root zone soil moisture on a tidal time scale. The first objective is addressed with a combination of site physical data and seasonal hydrologic data. The second objective is addressed by examining the relationship between tidal elevation and water table fluctuation within the upland region of the transect and by using a scaling exercise to examine the role of both soil texture and elevation in controlling the magnitude of tidal forcing effects on soil moisture dynamics.

2.2 METHODS

2.2.1 Site Description

The area chosen for this study is the Phillips Creek marsh (37° 27'N, 75° 50'W) located in Brownsville, VA, which lies within the Virginia Coastal Reserve (VCR/LTER) (Figure 2.2). The study area is a fringing tidal marsh on the mainland side of a coastal lagoon on the Eastern Shore of Virginia, with tidal flooding occurring from the southwest by Phillips Creek. The tidal range of Phillips Creek is approximately 1.5-2 m (Christiansen, 1998) and the average monthly rainfall for the Phillips Creek marsh is approximately 86 mm, with the maximum rainfall occurring during the summer months due to high intensity convective storms (USDA, 1989).

The study site is located within the Bell Neck complex which is comprised of agricultural and forested upland areas, freshwater and tidal wetlands, and tidal creeks (Mixon, 1985). The Wachapreague formation underlies the Bell Neck complex in the study area, serving as the unconfined aquifer in the system (Mixon, 1985). The Wachapreague formation is approximately 12 m thick at this location (Nuttle and Harvey, 1995). Groundwater is fed to Wachapreague formation by the underlying Yorktown aquifer. The Yorktown aquifer is approximately 45 m thick and extends westward beneath the Delmarva Peninsula and the Chesapeake Bay (Nuttle and Harvey, 1995). The mean piezometric head in the Yorktown aquifer at this location is approximately 1 meter above the annual mean water table elevation, indicating a significant net discharge of groundwater to the overlying unconfined aquifer system (Fetsko, 1989).

The dominant soil types in the region of the Delmarva Peninsula chosen for this study are the Chincoteague (low marsh), Magotha (high marsh), and Nimmo and Munden

(upland) (USDA, 1989). The Magotha soil is a deep, fine sandy loam that is poorly drained. Like the Magotha, the Nimmo series are also deep soils that are poorly drained. The Munden soils are considered moderately well drained and have a coarser texture than the Magotha and Nimmo soils (Hmieleski, 1994). Within the Phillips Creek marsh, the surface sediments in the high marsh region are predominantly in the silt and clay size fractions (Christiansen, 1998). The silt is primarily quartz particles while the clay sized particles are predominantly illite (Kastler, 1993). Harvey and Nuttle (1995) found that high marsh surface sediments (including sediments to a depth of 20 cm) in the Phillips Creek marsh have a bulk density of approximately 1.5 g/cm^3 , a porosity of 0.42, and an average organic content of 4% (average low marsh organic content in this marsh was found to be 6% by Kastler and Wiberg (1996)).

Within Phillips Creek marsh, distinctive and well-developed plant communities exist in each discrete zone along the gradient from tidal high marsh to forested upland. *S. alterniflora* (short form), *S. patens*, *D. spicata*, and the shrub species *I. frutescens* and *B. halimifolia* dominate the high marsh. The herbaceous species *S. patens* and *P. virgatum*, along with the shrub species *B. halimifolia* and *M. cerifera* and the tree species *P. taeda* and *J. virginiana* characterize the transition zone. In the upland fringe area of Phillips Creek, the ground cover is predominantly *R. radicans*, *Sagittaria larifolia*, and *P. virgatum*. The shrub species in the upland are mostly *B. halimifolia*, *M. cerifera*, and small *J. virginiana* and tree species in this region of the upland are *P. taeda* and *J. virginiana*. The percent cover of the ground cover vegetation and shrubs are low compared to tree species cover in the upland region investigated for this study (summarized from Hmieleski, 1994).

2.2.2 Field Study

2.2.2.1 Transect Designation

In order to study the hydrologic processes that occur across a marsh-upland transition, a transect was established perpendicular to the marsh-forest border in the Phillips Creek marsh in the summer of 1999 (Figure 2.3). The ground surface elevation was surveyed every meter to insure that microtopographic features (i.e., local depressions) would be represented, with the elevations referenced to the Hayden Benchmark (Virginia Coastal Reserve benchmark HAYD, N 372732.021 W 754958.036) located approximately 90 m northeast of the site. The study transect was approximately 16 m in length and spanned the distance from the upland edge of the high marsh (approximately 55 m from the tidal creek bank) to approximately 3 m into the upland forest. Boundaries of the transition zone within the study transect were determined by soil moisture and vegetation characteristics. The marsh edge of the transition zone was defined by the presence of *I. frutescens* (59 m from the creek bank) while the upland edge of the transition was defined by the location where average soil moisture indicated the existence of well-drained, upland soils (69 m from the creek bank).

The area of the Phillips Creek marsh chosen for investigation had a high degree of variability of tidal inundation along the transect and a relatively steep gradient from the high marsh to the upland (short distance along transition from marsh to forest), resulting in a distinct vegetative zonation between the high marsh, marsh-upland transition, and the upland. *S. alterniflora* (short form), *S. patens*, and *D. spicata* are dominant in the high marsh portion of the transect. A narrow region of *S. patens*, *D. spicata*, and the shrub *I. frutescens* characterizes the marsh edge of the transition zone. As elevation increases,

transition zone vegetation changes to a combination of *S. patens*, *D. spicata*, and the shrub *B. frutescens*, with both the forest edge of the transition zone and the upland fringe being characterized by the tree species *P. taeda* (loblolly pine) and *J. virginiana* (red cedar). The diameter at breast height (DBH) measurements for *P. taeda* and *J. virginiana* were on the order of 40 cm and 20 cm, respectively.

2.2.2.2 Soil Moisture Measurements

Soil moisture content of the near-surface root zone (top 30 cm) was monitored by an array of time domain reflectometry (TDR) probes (Campbell Scientific CS615) during the summer of 1999 (Figure 2.3). The study transect was instrumented with 16 probes that were spaced 1 meter apart, extending across the marsh-upland transition from the high marsh into the upland fringe. Each TDR probe output the wave period of an electromagnetic pulse from July 14 to August 13 (days 195-225). Probe output was recorded hourly on a Campbell Scientific 21X datalogger. Wave period was converted to soil moisture by correlating probe period output and measured volumetric soil moisture. Volumetric soil moisture content was determined periodically during the summer study period at each TDR probe location along the study transect by taking a soil core to a depth of 30 cm (using a 1 inch push core) and drying approximately 30 to 40 grams of the sample for 48 hours at 105° C in a forced air oven. The volumetric soil moisture content was determined for each sample as a product of the % soil moisture by mass and the dry soil bulk density divided by the unit weight of water. The % soil moisture by mass was calculated as the ratio of the difference between wet and dry soil weight to dry soil weight. Dry soil bulk density was calculated as the dry soil weight divided by soil bulk

volume (Tan, 1996). The calibration curve relating probe period to volumetric soil moisture for the probes along the transition from marsh to upland is given in [Appendix A](#).

2.2.2.3 Soil Properties

Samples taken for volumetric water content were split into two subsample sets and analyzed for bulk soil salinity and bulk organic content. The bulk salinity was determined by placing a homogenized dried soil sample in distilled water and measuring the electroconductivity of the filtered solution by means of a handheld conductivity meter (YSI Model 30). The electroconductivity measurements were then converted to salinity (ppt) using a standard calibration equation. Subsamples for organic matter determination were pre-weighed, burned in an ash oven for 3 hours at 500° C, and reweighed to obtain % bulk organic matter for the upper 30 cm of soil (Harvey, 1986).

In order to classify the soil texture within the study site, soil cores were obtained using a 3 inch diameter augur in July of 1999. Cores were taken adjacent to the transition and upland wells to a depth of 1.5 m. The depth to different soil layers was determined qualitatively, however it was apparent where there was a significant change in soil type. Textural properties of each soil sample collected were quantified in the laboratory using the hydrometer method (ASTM, 1981). The hydrometer method allowed the density of a soil-water-dispersant (1 M Sodium hexametaphosphate) solution at an increasing time interval to be measured so that the soil type could be determined by the weight percent of sand, silt, and clay and.

Hydraulic properties (θ_s , K_s , b , Ψ_s) of the soils present were determined from the % sand and % clay of each soil by means of an empirical pedotransfer function (PTFs)

derived by Saxton *et al.* (1986). The PTFs used to calculate the hydraulic variables were:

$$q_s = 0.332 - [7.251 \times 10^{-4} (f_s)] + [0.1276 \log_{10} (f_c)] \quad (2.1)$$

$$K_s = 2.778 \times 10^{-6} (\exp\{12.012 - [7.55 \times 10^{-2} (f_s)] - [3.8950 + 3.671 \times 10^{-2} (f_s) + 0.1103 (f_c) - 8.7546 \times 10^{-4} (f_c)^2] (1/q_s)\}) \quad (2.2)$$

$$b = -3.14 - [2.22 \times 10^{-3} (f_c)^2] - [3.484 \times 10^{-5} (f_s)^2] - [3.484 \times 10^{-5} (f_s)^2 (f_c)] \quad (2.3)$$

$$\Psi_s = (\exp\{-4.396 - [0.0715 (f_c)] - [4.880 \times 10^{-4} (f_s)^2] - [4.285 \times 10^{-5} (f_s)^2 (f_c)]\} 100) (q_s)^b \quad (2.4)$$

where f_s is the percent sand, f_c is the percent clay, q_s is saturated soil moisture, K_s is saturated hydraulic conductivity (m/s), b is an empirical parameter, and Ψ_s is saturated matric potential (kPa). Current research (i.e., Montaldo and Albertson, 2001) has shown renewed interest in the Saxton *et al.* (1986) PTFs due to their ease of implementation and broad range of applicability. These equations give useful estimates of soil hydraulic properties for typical soil tension values where sand content is greater than 5% and clay content ranges between 5% and 60%.

2.2.2.4 Water Table Elevation

The depth of the unsaturated zone at the marsh edge of the transition zone (60 m from the adjacent tidal creek) and the upland fringe (70 m from the adjacent tidal creek) was measured through the use of 3 in. diameter wells installed to a depth of 1.5 m. Water table elevations were measured daily at each well during low tide using a hand-held salinity/electroconductivity sensor (YSI Model 30) during the summer field study (days 195-225). Daily water table measurements were taken at low tide to get an indication of

water table position with a low degree of tidal influence. To examine tidal-scale fluctuations in water table elevation along the transect, the water table elevation at the upland fringe well was recorded at a 5 minute interval from days 221.8-224.5 through the use of automated well loggers (Soilinst M5). During a period in December 1999 (days 335-355), the well at 70 m was logged on a 15 minute time interval. The complete methodology for water table measurements is given in Turaski (2001).

2.2.2.5 Tidal Elevation and Tidal Inundation

The degree of tidal inundation on the study transect during the summer study period was characterized by tidal elevation in Phillips Creek marsh adjacent to the study site. Tidal elevation for the region of Phillips Creek marsh under investigation was calculated by use of hourly tide data provided by the NOAA tide gage in Wachapreague (located approximately 20 km north of the transect). In order to obtain tidal elevation within the Phillips Creek marsh, the Wachapreague tidal elevations were converted to tidal elevations at Redbank (located south of Phillips Creek) by adding .185 m to the tidal elevation. Redbank tidal elevation was then converted to tidal elevation within Phillips Creek marsh by use of an empirical relationship by Christiansen (1998):

$$wl_{pc} = wl_{rb} * 1.08 - 1.99 \quad (2.5)$$

where wl_{pc} is the Phillips Creek tidal elevation (meters above MSL [mean sea level]) and wl_{rb} is the tidal elevation at Redbank. The mean difference between tidal elevation predicted by the Christiansen (1998) equation and tidal elevation on the study transect is 0.04 m (Turaski, 2001). Tidal inundation frequency for elevations along the study

transect during the summer study period was then determined from tidal elevation as the total amount of time that the tide was at or above a given elevation on the study transect.

2.2.2.6 Meteorological Processes

Measurements of meteorological variables were made in the Phillips Creek marsh to quantify the degree of export of pore water (evapotranspiration) and input of pore water (precipitation) due to atmospheric forcing. Hourly values of soil heat flux (Campbell Scientific HFT) were measured within the transition zone at a depth of 7 cm. Values of hourly photosynthetically active radiation [PAR] (Li-Cor 190S), air temperature (Campbell Scientific HMP35C) and precipitation (Campbell Scientific TE525) were measured by a micrometeorological station within Phillips Creek marsh that is maintained by the LTER station in Oyster, VA. All values were recorded on a Campbell Scientific 21X datalogger.

The evapotranspiration for the study site was estimated from the meteorological variables by use of the Priestly-Taylor (1972) formula for potential evapotranspiration. The Priestly-Taylor formula gives the rate of evapotranspiration as an expression of the latent heat flux density:

$$LE = \alpha \left(\frac{s}{s + \gamma} \right) (R_n - G) \quad (2.6)$$

where α is an empirical constant (1.26), s is the rate change of saturation vapor pressure with local air temperature, γ is the psychrometric constant (ratio of sensible heat content of air to latent heat content of water vapor in vapor-saturated air), R_n is the net radiation flux to the ground surface, and G is the soil heat flux (Priestly and Taylor, 1972).

Previous research has shown that the Priestly-Taylor expression is appropriate for

estimating evapotranspiration in tidal wetland environments (Nuttle and Hemond, 1988; Price and Woo, 1988; Nuttle and Harvey, 1995).

2.3 RESULTS AND DISCUSSION

2.3.1 Overview

This section gives a physical description of the study transect (vegetation zonation, soil properties, pore water properties) and values of hydrologic input variables (atmospheric forcing and tidal elevation) during the summer field campaign. Elevation controls on water table elevation and the spatial and temporal evolution of near-surface soil moisture on a seasonal time scale are discussed. Time series of water table elevation and tidal elevation for the summer study period and for a winter study period are used to determine the affect of tidal forcing on water table elevation on a tidal time scale. Finally, a scaling approach is used to examine the role of elevation and soil texture on tidally induced water table rise into the unsaturated zone and the magnitude of the effects of tidal forcing on soil moisture within coastal environments.

2.3.2 Site Variables for Summer Study Period

Time series of hydrologic variables affecting soil moisture dynamics on the Phillips Creek marsh site during the summer study period (days 194.5-225) are shown in [Figure 2.4](#). Average daily maximum potential evapotranspiration during the study period was 1.14 mm/hr (.0019 cm/min), which is comparable to the average daily maximum potential evapotranspiration measured by Nuttle and Harvey (1995) during summer months on the Phillips Creek marsh. Precipitation events during the study period were

characterized by sporadic, short duration storms. Maximum tidal elevation was 1.43 meters above MSL (reached on day 194.9), with average high tide for the study period 0.81 m above MSL. Inundation frequency during the study period increased exponentially from the upland fringe to the edge of the high marsh (Figure 2.5). Values for inundation frequency ranged from 4.5% of the study period at the high marsh edge of the transition zone (probe 16) to .01% of the study period at the upland edge of the transition zone (probe 4). Tidal water did not reach probes 1 through 3 during the summer study period.

Average pore water salinity for the top 30 cm of soil along the study transect increased linearly from the upland fringe to the high marsh during the summer study period (Figure 2.6). Values for average pore water salinity ranged from 7 ppt in the upland fringe to 35 ppt at the high marsh edge of the transition zone. The measurements of pore water salinity used in averaging show the variability of pore water along the transition zone as a function of tidal and precipitation inputs. In general, the pore water salinity values taken along the transition zone three days after inundation to 1.43 meters above MSL (day 202) were highest. Pore water salinity measured on day 208 was generally the lowest along the transition from marsh to upland due to the high intensity/short duration storm on day 203 where 3.8 cm of rain was delivered to the marsh in 2 hours.

Soil texture along the transect was characterized by sandy loam basal sediments underlying a loam layer ranging in thickness from 0.7-0.8 m, with a thin organic layer in the upland fringe. The sand and clay content within the loam layer varied with vertically and laterally across the transition from marsh to forest (Table 2.1). Within the transition zone, surface loam sediments lie above a lower conductivity loam layer. The upland

fringe loam is vertically homogeneous, with a higher sand content than the transition and similar clay content. Organic matter contents for the top 30 cm of soil increased exponentially along the study transect (Figure 2.7). Organic matter ranged from 3% of the soil by volume at the high marsh edge to 7% of the soil by volume in the upland fringe. The decrease in organic matter content with a decrease in elevation corresponds to the change in vegetation and subsequent surface soil texture that occurs along the marsh-upland transition. The change in vegetation type from upland tree species to shrub species decreasing from 1.49-1.13 meters above MSL corresponds to a decrease in organic layer thickness and associated decrease in organic matter content by a factor of 2. From 1.13-0.81 meters above MSL, the change in vegetation from shrub species to marsh grass and the associated mineral surface soil along the decrease in elevation caused in a the organic content to decrease by a factor of 1.4.

The average low tide water table along the transition from marsh to upland for days 195-225 during the summer of 1999 exhibited a gradient where the marsh was discharging pore water to the upland (Figure 2.8). Average water table elevations taken at low tide indicate water table at 0.79 m above MSL at the transition well and water table at the upland well was at an elevation of 0.46 m above MSL during low tide for the summer study period. The hydraulic gradient observed at the study site is in accordance with hydraulic gradients measured by both Harvey (1986) and Hmieleski (1994) along a marsh-upland transition during summer months. Low precipitation input to the site during the study period (7.6 cm in 30 days) resulted in seasonally low infiltration and recharge further upland and a low average water table elevation within the upland fringe. The water table elevation within the transition zone remained above the upland fringe

water table due to the increase in tidal inundation within the lower elevations of the marsh-upland transition.

2.3.3 Control on Seasonal Soil Moisture Dynamics along the Transect

2.3.3.1 Soil Moisture Time Series

The time series of soil moisture along the transition from marsh to upland during the summer study period is shown in [Figure 2.9](#). Along the entire transect, depth-averaged volumetric soil moisture for the top 30 cm of soil ranged from 15% to 40%. In general, the upland fringe (68.2-70.3 meters from the creek bank) remained well drained for the duration of the summer study period while the portion of the transect from 62.1-55 meters from the creek bank remained close to saturation. Variation in soil moisture for each location along the study transect remained low. The average difference between minimum and maximum volumetric soil moisture for each location on the study transect during the summer study period was 10%.

2.3.3.2 Elevation Control on Seasonal Soil Moisture Dynamics

The trend in seasonal soil moisture along the transition from marsh to upland suggests a relationship such that soil moisture responded to changes in elevation. The increase in elevation along the study transect corresponded to changes in both average soil moisture content and the variability in soil moisture for the study period. To assess the role of elevation in controlling soil moisture dynamics on a seasonal time scale, mean soil moisture content and soil moisture variance along the study transect were examined as functions of surface elevation ([Figure 2.10](#)). Understanding elevation controls on soil

moisture dynamics along the transition from marsh to upland can be crucial in determining areas that are saturated on average on a seasonal time scale.

The relationship between average soil moisture and elevation changes as surface elevation increases from the marsh edge to the upland fringe (Figure 2.10a). For lower elevations on the study transect, there is no significant relationship between average soil moisture for the summer study period and surface elevation. Average soil moisture remained at 40% for an increase in surface elevation of 0.85-1.20 meters above MSL. Between surface elevations of 1.20 and 1.48 meters above MSL, average soil moisture shows a statistically significant linear trend where average soil moisture decreased from 40-15% ($R^2=0.89$). This trend in average soil moisture with an increase in surface elevation corresponds to the trend in average low tide water table with increasing surface elevation during the study period (Figure 2.8). Between the high marsh and well 60 (1.14 meters above MSL), average low tide water table showed a low degree of variation (0.74 meters above MSL in the high marsh and 0.79 meters above MSL at well 60). The increase in surface elevation from well 60 to well 70 (1.48 meters above MSL) resulted in a decrease in average low tide water table elevation from 0.79-0.46 meters above MSL. Overall, average soil moisture remained constant from 0.79-1.20 meters above MSL and decreased from 1.20-1.48 meters above MSL due to the average thickness of the unsaturated zone during the time period when the soil moisture measurements were taken. Therefore, the average water table depth associated with an increase in surface elevation along the transition from marsh to upland significantly contributed to the control of the seasonal soil moisture during the summer study period.

The variability of soil moisture along the marsh-upland transition zone during the summer study period increased with an increase in surface elevation (Figure 2.10b). The coefficient of variance of soil moisture measurements shows a statistically significant exponential increase as surface elevation increased from the high marsh to the upland fringe ($R^2=0.57$). On average, the proximity of the average water table to the ground surface controlled the variation in soil moisture. High average water table at the lower surface elevations resulted in saturated soils and low soil moisture variability and low average water table in the upland fringe caused surface soils to be drier with a higher degree of soil moisture variability. Although water table elevation was the primary control soil moisture variability, factors such as microtopography and surface textural heterogeneity along the transition were also contributing to soil moisture variability and contributed to the scatter of the variance-surface elevation relationship. For example, the low organic content relative to the upland fringe (see Figure 2.7) and microtopographic low 1.30 meters above MSL (see Figure 2.3) resulted in slow return to field capacity after tidal inundation and an associated high coefficient of soil moisture variability. For the lower surface elevations along the study transect, the effect of soil surface heterogeneity on soil moisture variability was decreased due to water table effects keeping the surface soil close to saturation for the entire summer study period.

The role of water table elevation in controlling soil moisture dynamics along the marsh-upland transition on a seasonal time scale is evident from the relationship between surface elevation and seasonal soil moisture characteristics. Fluctuation of water table elevation by tidal forcing within the marsh-upland transition zone has implications for affecting soil moisture dynamics on a tidal time scale. The next section first explores the

relationship between tidal elevation and water table fluctuation within the upland fringe, and then examines the role of texture and elevation on controlling tidally induced water table fluctuations and soil moisture dynamics within the tidal environments.

2.3.4 Controls on Tidal Time Scale Soil Moisture Dynamics

2.3.4.1 Tidal Time Scale Water Table Fluctuations within the Upland Fringe

To examine the role of tidally induced water table fluctuations on soil moisture dynamics within the marsh-upland transition, the control of tidal elevation on the magnitude of water table fluctuations within the upland fringe was first determined. Tidal elevation and water table elevations at well 70 for days 221-224 (summer study period) and days 336-355 (winter study period) are given in [Figure 2.11](#). For the summer study period, average water table rise by tidal forcing was 0.12 m, average high tide elevation was 0.90 m above MSL, and the average lag between high tide and maximum water table elevation was 65 min. For the winter study period, average tidally induced water table rise was 0.06 m, average high tide was 0.6 m above MSL, and average lag time was 19 minutes. Tidally induced water table fluctuations in this environment occur 50 meters beyond the distance recorded by Hughes *et al* (1998) for the maximum extent of salt marsh water table fluctuations. The hydraulic characteristics of the sandy loam layer at depth are suggested to help facilitate the tidal forcing effects on water table fluctuations into the upland fringe 70 meters from the tidal creek.

The control of tidal elevation on the magnitude of water table fluctuations in the upland fringe is shown in [Figure 2.12](#). The range in high tide elevation from 0.07-1.12 meters above MSL corresponds to a range in water table fluctuations range from 1-17

cm. The data for the summer and winter study periods capture the water table fluctuations for the 0.5-1.0 meter above MSL range of predicted astronomical tides for Phillips Creek (Christiansen, 1998). The relationship between high tide elevation and water table rise for high tide elevation between 0.07 and 1.12 meters above MSL is essentially linear ($R^2=0.85$). For the upland fringe, the extent that the water table can rise and thereby affect soil moisture is a linear function of the high tide elevation within the tidal creek. The difference between water table rise in the sandy loam layer and water table rise in the loam layer for the same high tide elevation was small. Although the value for K_s for the loam layer was approximately half the K_s for the underlying sandy loam, the low degree in water table fluctuation variability among the soil layer for the same tidal elevation suggests that the sandy loam layer mediated the tidal control on water table fluctuation for the soil column. In general, soil hydraulic properties are suggested to determine the control of tidal forcing on water table fluctuations within the upland fringe.

The effect of tidal forcing on water table fluctuation has been shown to be a linear function for the soil conditions and elevation above MSL within the upland fringe. The magnitude of both the soil hydraulic conductivity and the elevation above MSL can be considered the important factors for determining the degree to which the tidally induced water table fluctuations in this environment can affect soil moisture dynamics. The following analysis explores the role of both soil texture and elevation in controlling the magnitude of tidal importance on soil moisture dynamics within tidal environments.

2.3.4.2 Tidal Importance in Controlling Soil Moisture Dynamics

Tidal forcing contributes to the control of soil moisture dynamics by causing water table rise into the unsaturated zone. Factors important in determining the effects of tidal forcing on soil moisture in tidal environments are the conductivity of the soil and the elevation of the water table in relation to the soil surface. In the analysis presented in this section, both hydraulic conductivity and an elevation term are varied to determine the variability of the magnitude of tidal importance on soil moisture dynamics. Examining the tidal importance on soil moisture dynamics in this environment can be significant in contributing to the overall understanding of soil saturation in coastal environments.

To examine the magnitude of the water table response to tidal forcing, a length scale of tidal influence on water table fluctuations (h_t) was determined as a function of a soil response velocity scale and tidal time scale. The expression for the length scale of tidal influence on water table forcing can be expressed as

$$h_t = K_s * T \quad (2.7)$$

where K_s is saturated hydraulic conductivity (cm/min) and T is tidal period (min). In this analysis, saturated hydraulic conductivity was used as an indicator of soil texture. Tidal period used for determining h_t 780 minutes (13 hours). The value for h_t can be considered a maximum water table response to tidal forcing over one tidal period. An index of the importance of tidal forcing on soil moisture (F_t) was then determined as a function of h_t and an elevation term. The F_t value was determined by the expression

$$F_t = \frac{h_t}{d} \quad (2.8)$$

where d is water table depth (cm). For this investigation, water table depth was used as a proxy for elevation. Field measurements from this study and from previous studies

(Harvey, 1986; Hmieleski, 1994) show an increase in average water table depth with an increase in elevation from the marsh to the upland, suggesting the validity of water table depth as a surrogate for elevation. To determine a range of the magnitude of tidal forcing importance on soil moisture dynamics, K_s and d were both varied by an order of magnitude. The value of F_t can be considered the maximum magnitude of tidal forcing affects on unsaturated zone soil moisture for prescribed textural and elevation characteristics. In general, a higher value of F_t corresponds to a greater degree of the unsaturated zone affected by tidally induced water table fluctuations.

The effects of varying both soil texture and elevation on the magnitude of the importance of tidal forcing on soil moisture dynamics are shown in [Figure 2.13](#). The scaling of both K_s and d resulted in zones of similar tidal importance on soil moisture where the range of the higher and lower F_t magnitudes was small. Considering an increase in water table depth to be an indication of an increase in distance from the tidal creek, tidal influence on soil moisture is greatest for high conductivity soils close to the tidal signal. Over one tidal period, high conductivity soils and a shallow unsaturated zone characteristic of regions closest to the tidal creek cause tidally induced water table fluctuations to have the greatest effect on soil saturation dynamics. The magnitude of the importance of tidal forcing on soil moisture dynamics is similar for regions both close to the tidal signal with low conductivity soils and far from the tidal signal with high conductivity soils. Due to the scaling of K_s and d , high conductivity soils with a deep unsaturated zone and low conductivity soils with a shallow unsaturated zone have F_t values that are an order of magnitude lower than the highest F_t value determined. As distance from the tidal signal increases and soil hydraulic conductivity decreases, tidal

influence on soil moisture dynamics becomes less important. The F_t for the low conductivity soils with a deep water table is essentially two orders of magnitude lower than F_t for regions closest to the tidal source with the highest conductivity soil considered. Overall, the interaction between soil conductivity and elevation mediates the effect that tidal forcing can have on soil moisture dynamics within coastal environments adjacent to a tidal signal.

2.4 CONCLUSIONS

The control that elevation and soil texture have on soil seasonal moisture dynamics along the transition from a high marsh to an upland forest is variable both spatially and temporally. On a seasonal time scale, soil moisture dynamics in this environment were strongly influenced the decrease in water table elevation associated with an increase in surface elevation. Average soil moisture during the study period along the marsh-upland transition correlated with the average water table elevation. Tidal forcing kept the average water table elevation at the high marsh end of the transect elevated while low seasonal precipitation input caused a low average water table elevation within the upland fringe. Variability of seasonal soil moisture along the marsh-upland transition correlated well with elevation, however the variability in soil moisture did not correspond to water table elevation to the same degree as the as average soil moisture. Surface soil textural heterogeneity and microtopographic influences resulted in the variability in the relationship between soil moisture variance and surface elevation.

On a tidal time scale, soil texture and elevation mediate tidally induced water table fluctuation and the role of tidal forcing on soil moisture dynamics along a marsh-upland

transition. Within the upland fringe, water table response to high tide elevation was linear. Soil texture in essence mediated the control of water table fluctuation for a given elevation along the marsh-upland transition. Exploring the control of both soil texture and elevation on soil moisture by tidally induced water table fluctuations illustrated the sensitivity of tidal control on soil moisture dynamics. An index of tidal importance on soil moisture was devised that utilized hydraulic conductivity and elevation. Varying both saturated hydraulic conductivity (texture term) and water table depth (elevation term) by an order of magnitude in the index of tidal importance formulation showed the variability in magnitude of possible tidal effects on soil moisture for different soil textures and positions from the tidal signal. High conductivity soils close to the tidal signal (low water table depth) had the highest possible degree of tidal effects on soil moisture. Low conductivity soils close to the tidal signal and high conductivity soils farther from the tidal signal had the same magnitude of possible tidal effects on soil moisture dynamics. Positions far from the tidal signal with low conductivity, similar to the upland fringe well location, had the lowest degree of possible tidal influence on soil moisture. Combining results from this analysis with previous work such as the formulation of tidal signal attenuation with distance from the tidal signal devised by Li *et al* (2000a) could further the prediction of soil moisture in tidal environments in general. Understanding the controls on the magnitude of water table rise as a function of distance from the tidal signal can be used to then better estimate the effects that water table fluctuations can have on soil moisture dynamics over a tidal period.

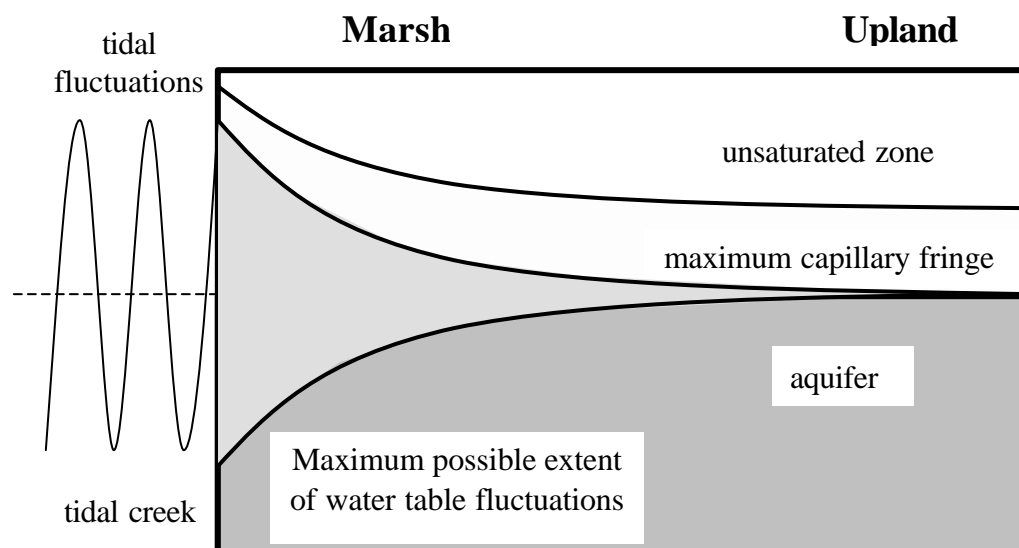


Figure 2.1 Schematic diagram representing water table fluctuations by tidal forcing in coastal environments. (From Li *et al.*, 2000c)

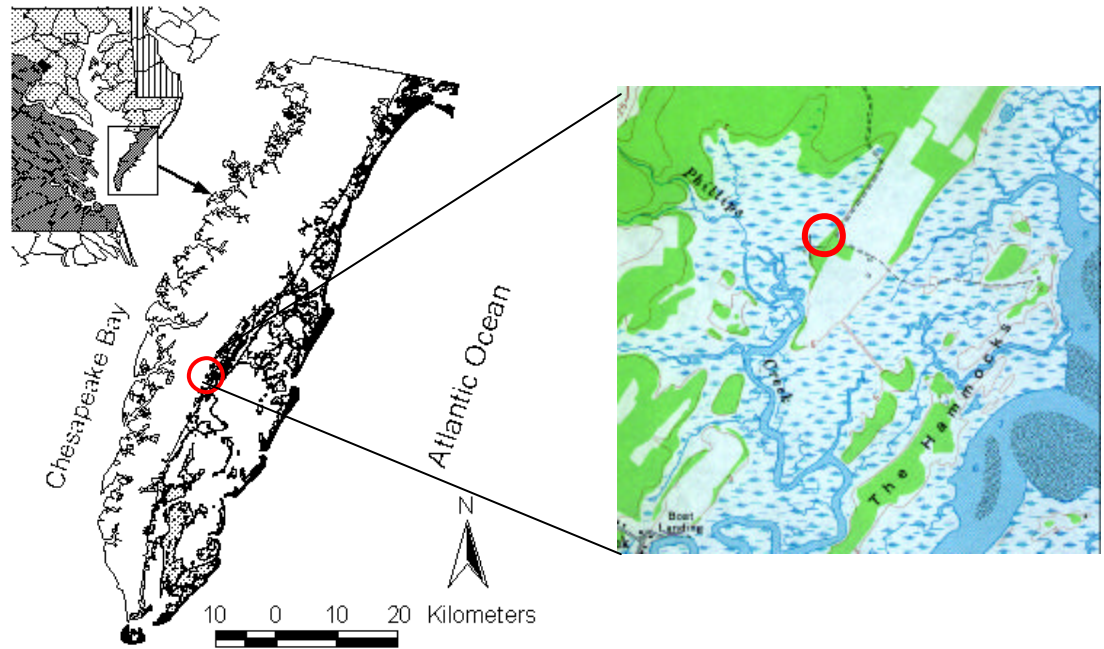


Figure 2.2 Location of the study site within Phillips Creek marsh on the Eastern Shore of Virginia. The transect location is indicated by the bold red circle.

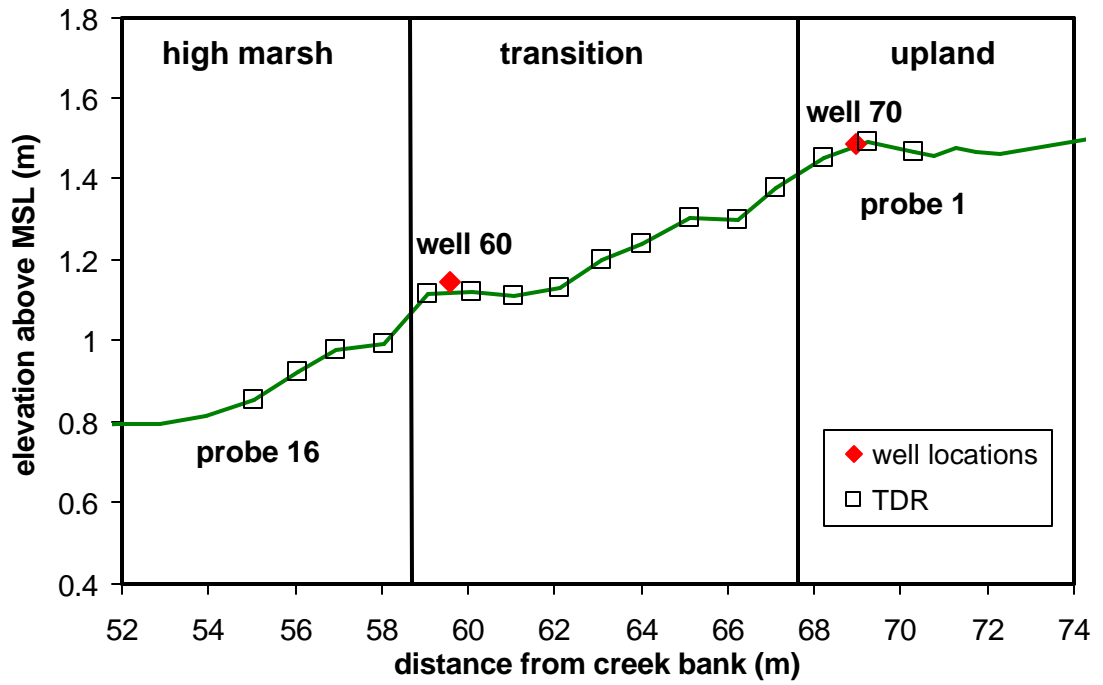


Figure 2.3 Longitudinal profile of the study transect with zone delineation and instrument location.

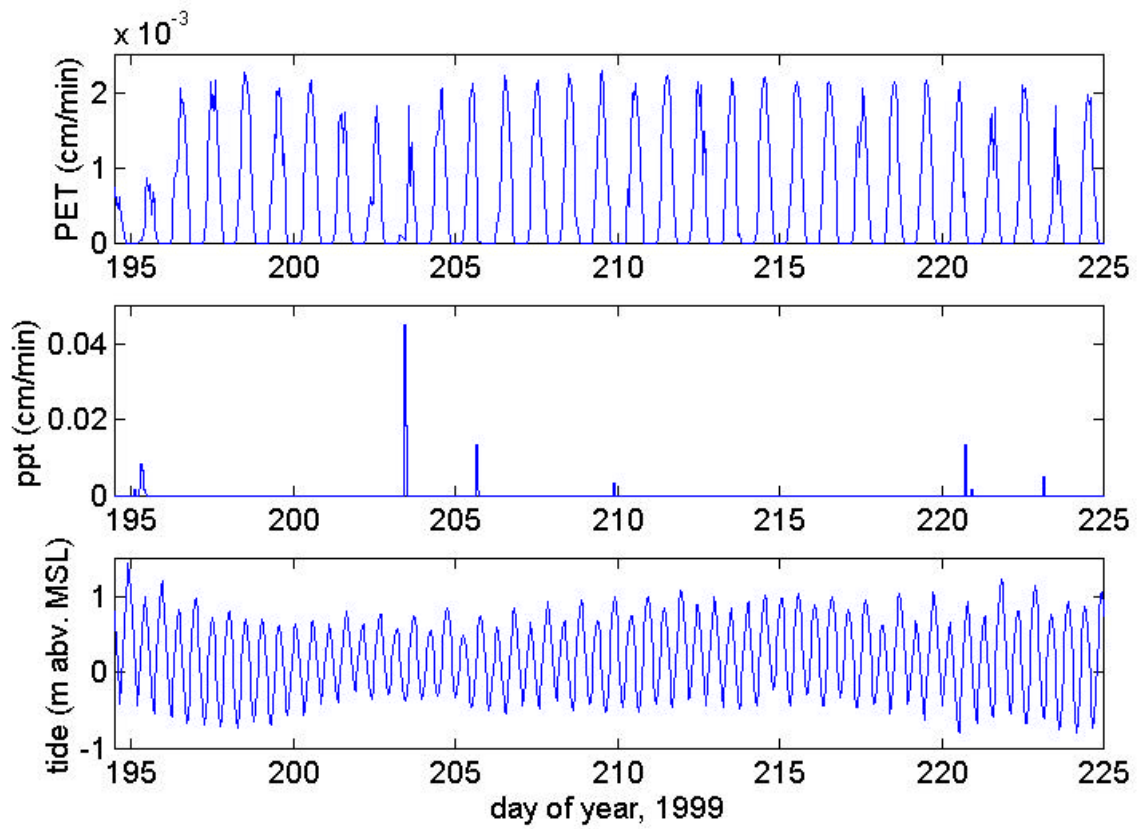


Figure 2.4 Hydrologic variables for Phillips Creek marsh during the summer of 1999.

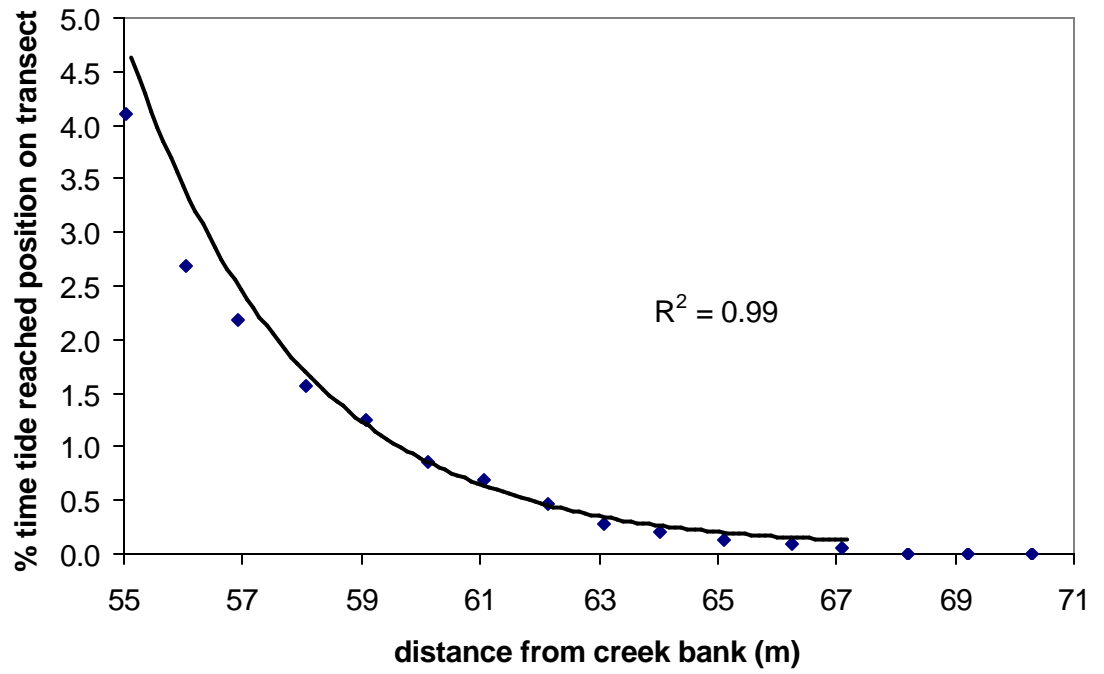


Figure 2.5 Inundation frequency along the study transect for days 194.5 to 225, 1999.

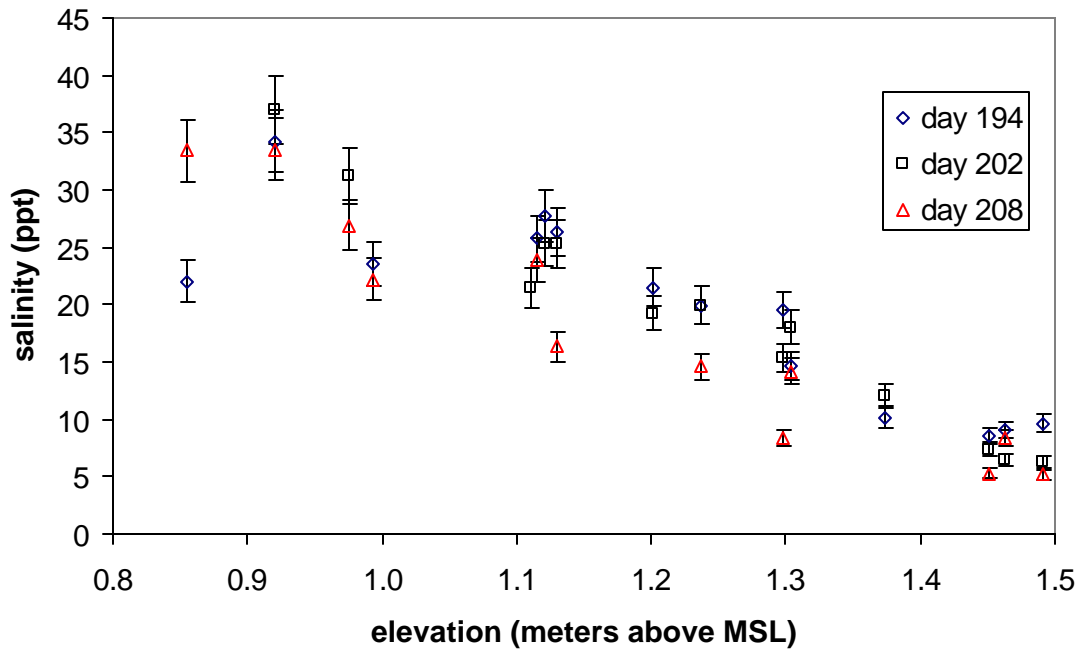
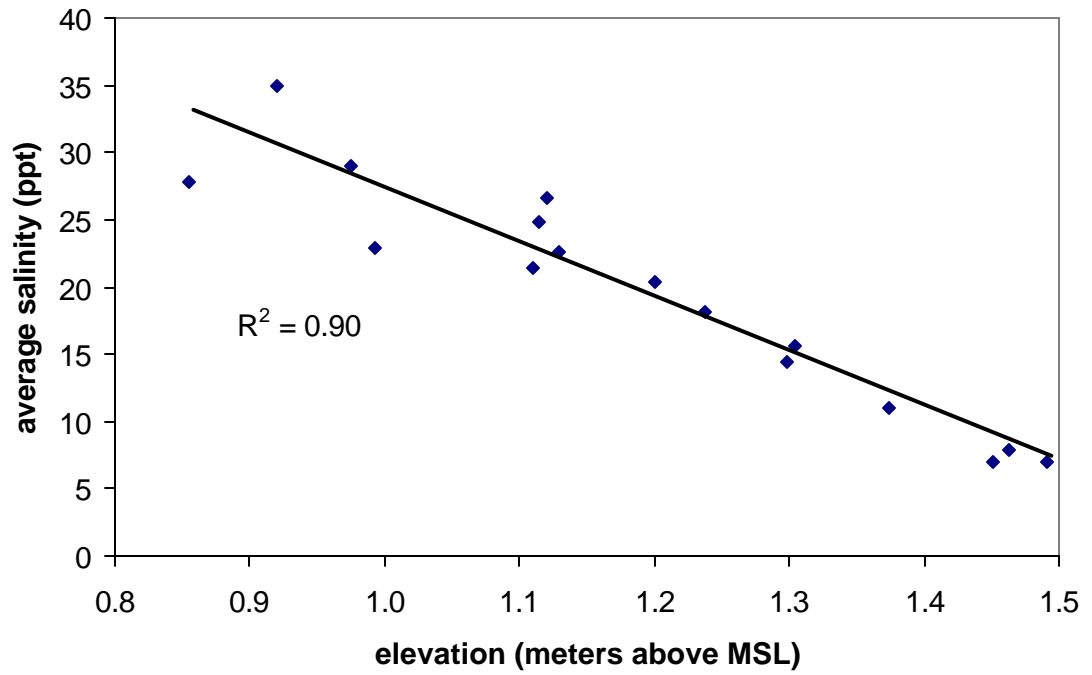


Figure 2.6 Pore water salinity for the top 30 cm of soil along the study transect during the summer of 1999. Error bars for daily salinity measurements represent a standard error of 8%.

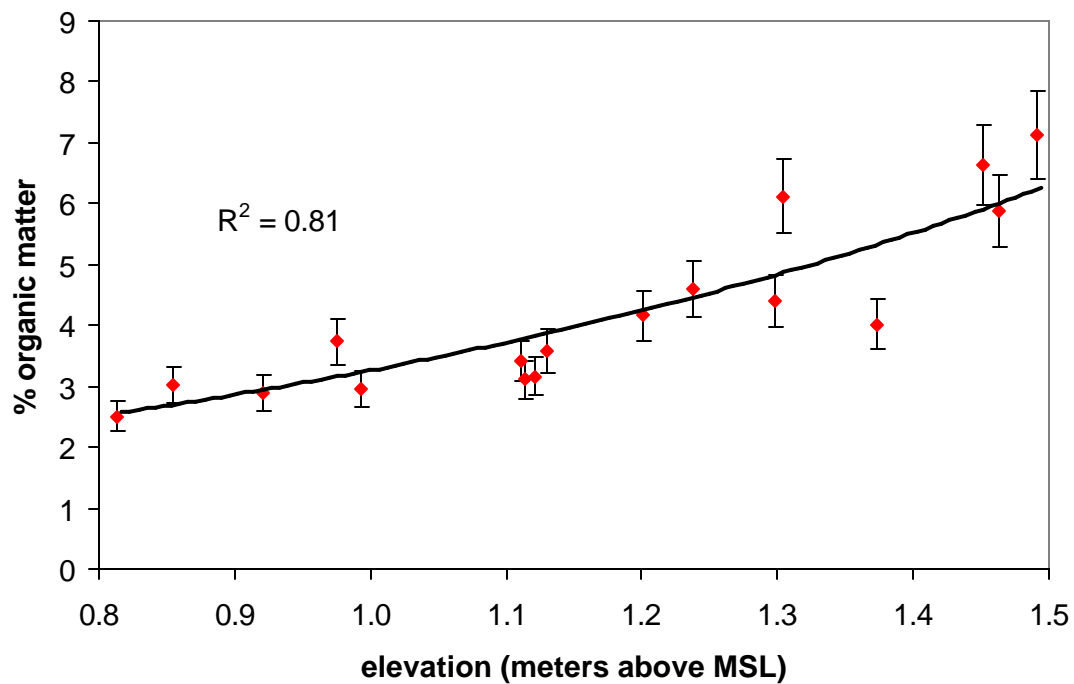


Figure 2.7 Organic matter content for the top 30 cm of soil during the summer of 1999. Error bars represent a standard error of 10% of % organic matter.

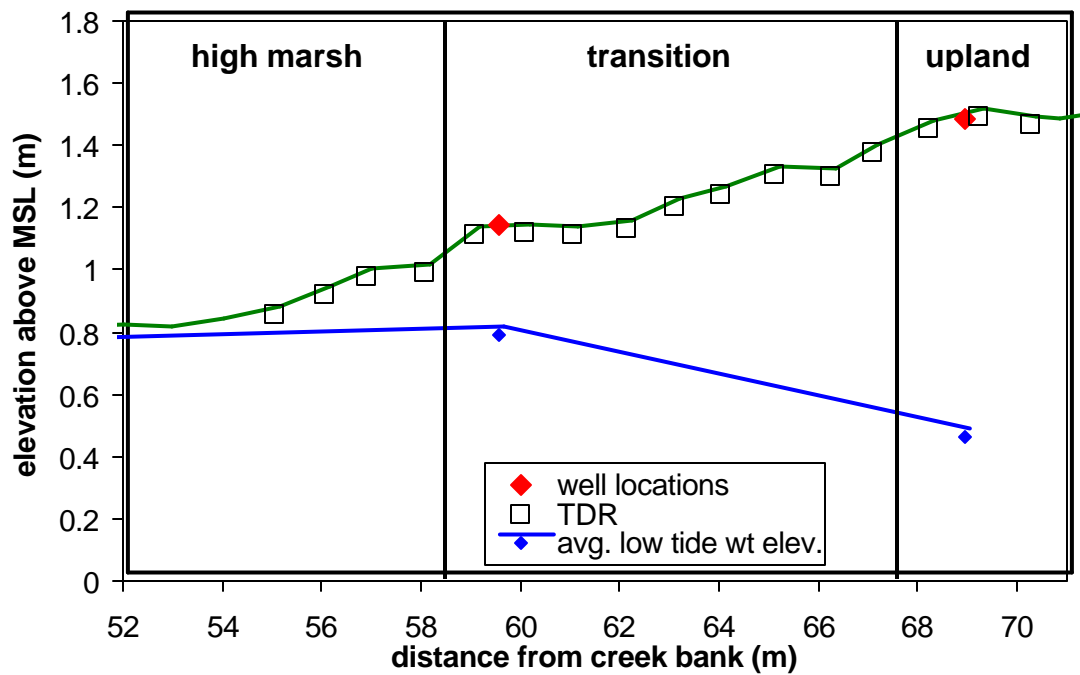


Figure 2.8 Average water table elevation for the well 60 (transition zone) and well 70 (upland fringe) from days 194 to 225, 1999. Error for well measurements was ± 1 cm.

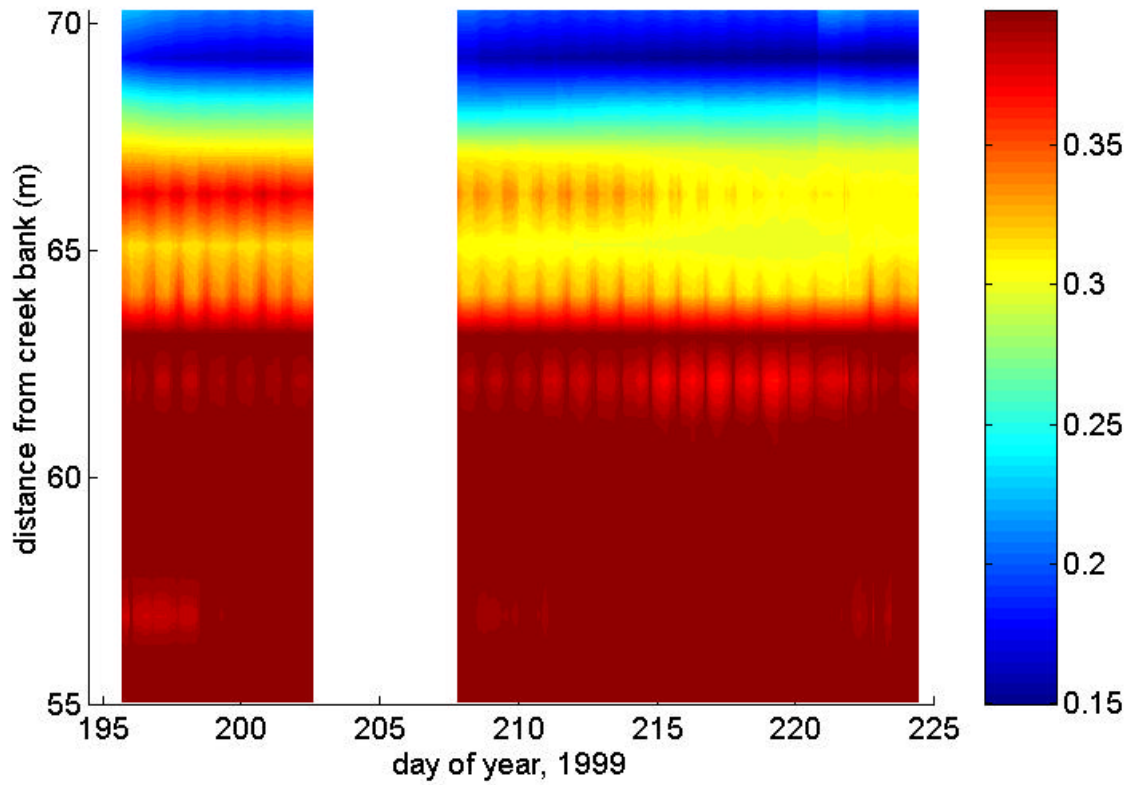


Figure 2.9 Time series of depth-averaged volumetric soil moisture for the top 30 cm of soil along the study transect during the summer of 1999. Gaps in the dataset (i.e, days 202-207) were caused by instrument malfunction.

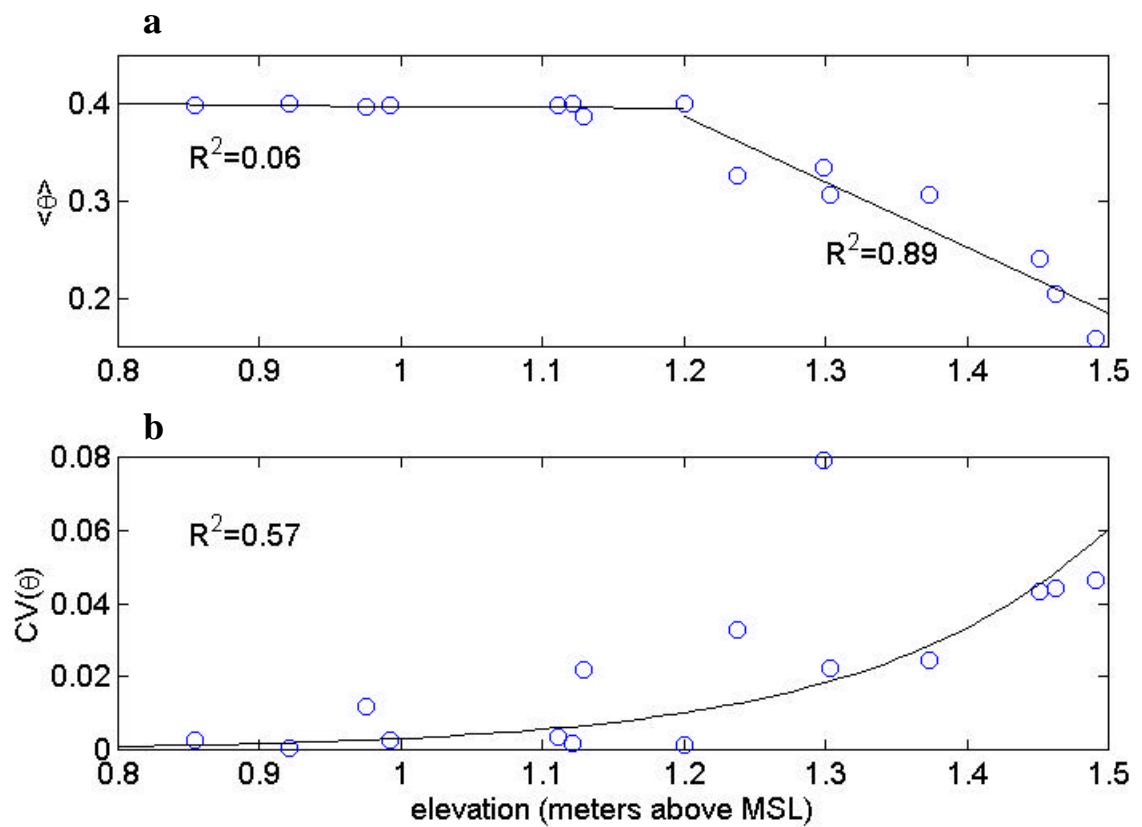


Figure 2.10 Time-averaged soil moisture ($\langle \theta \rangle$) and soil moisture variance ($CV(\theta)$) for the top 30 cm of soil along the study transect during the summer of 1999. The soil moisture variance (coefficient of variance) was determined by the expression $CV(\theta) = \sigma_{\theta} / \langle \theta \rangle$, where σ_{θ} is the standard deviation of the soil moisture time series.

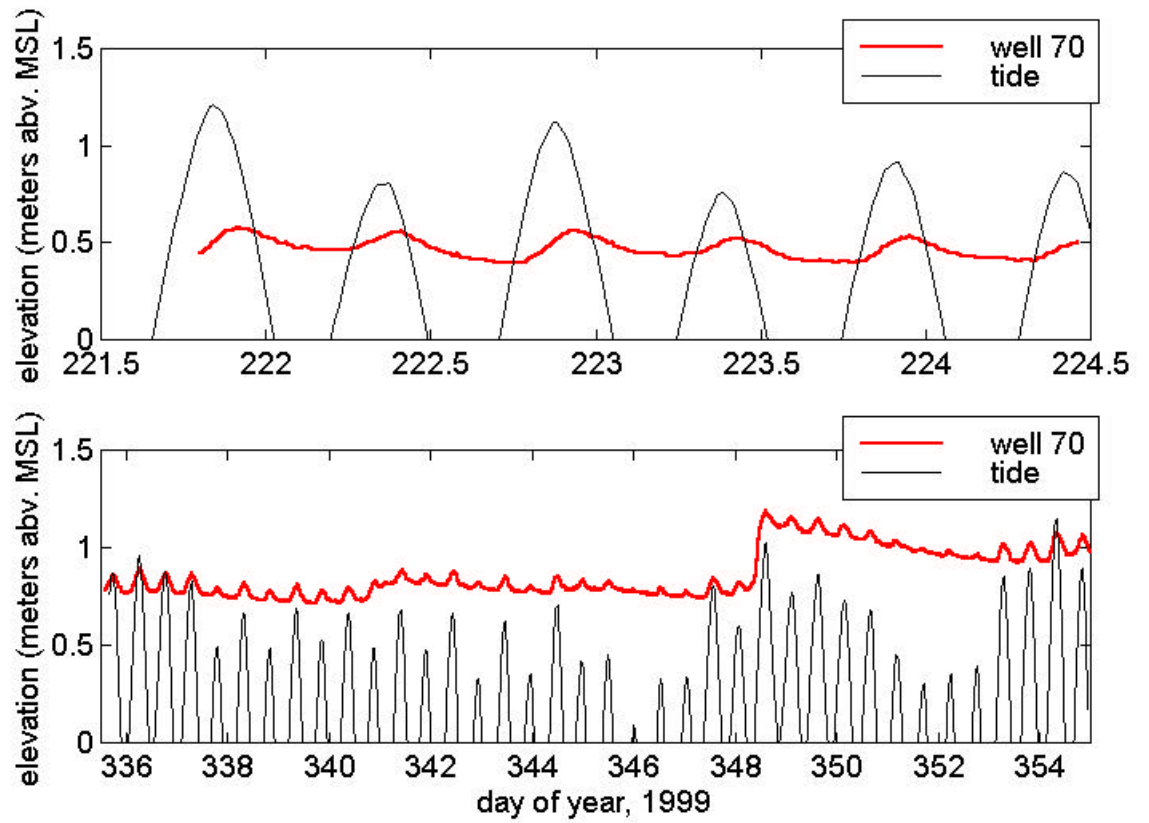


Figure 2.11 Time series of water table elevation in the upland fringe and tidal elevation for two study periods (summer and winter) in 1999. Error for water table measurements was on the order of ± 4 cm.

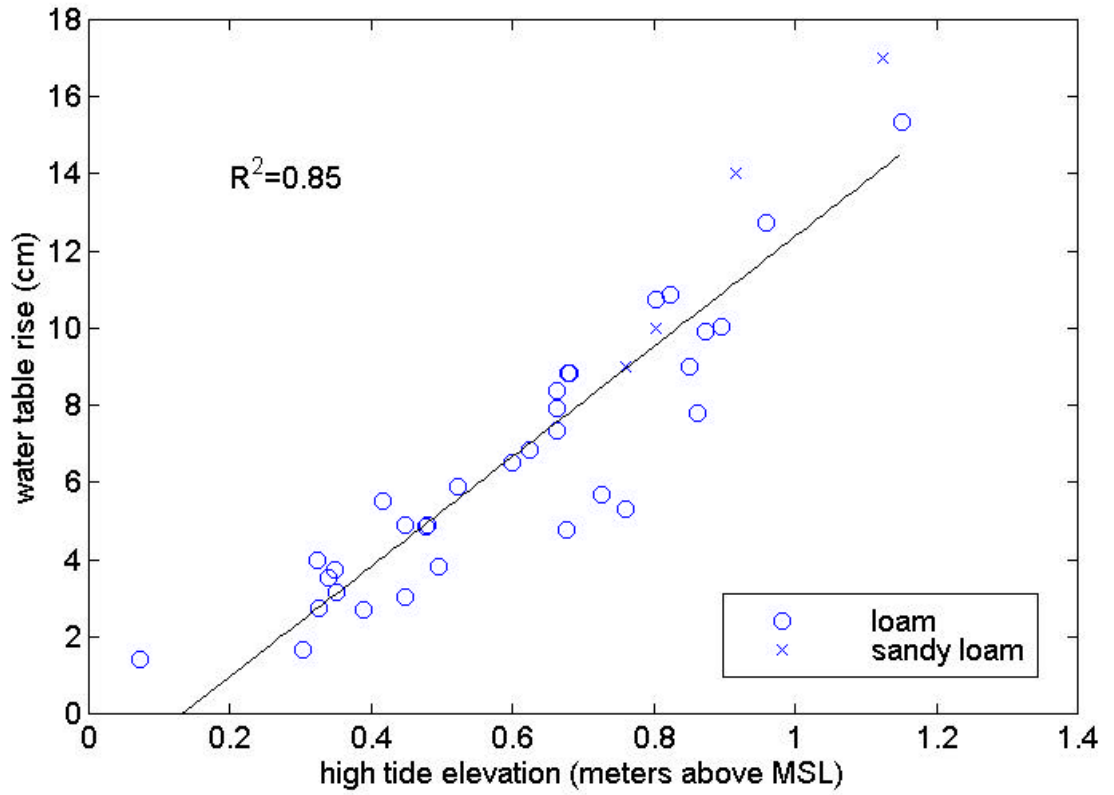


Figure 2.12 Tidally forced water table rise at well 70 with associated high tide elevation. Water table rise for when the water table was in the loam and sandy loam layer is represented.

Distance from creek bank (m)	Depth (cm)	Soil type	%sand	%clay	θ_{sat}	K_{sat} (cm/min)	b	Ψ_{sat} (-cm)
60	0-15	loam	44	17	0.46	0.0194	5	18
	16-30	loam	50	13	0.44	0.0300	4.7	18
	31-70	loam	36	22	0.48	0.0124	5.3	20
	71-100	sandy loam	71	14	0.37	0.0253	6.2	4
70	0-12	organic layer	--	--	0.35	0.0690	2.0	5
	13-60	loam	52	14	0.44	0.0260	5.0	15
	61-80	loam	50	20	0.46	0.0130	5.9	10
	81-100	sandy loam	75	9	0.40	0.0540	5.3	6

Table 2.1 Soil type with depth and associated soil hydraulic properties for the transition zone and upland fringe.

Chapter 3: The Role of Soil Texture and Vegetation Rooting Characteristics in Controlling Near-Surface Soil Moisture Dynamics Within Coastal Regions

3.1 INTRODUCTION

Understanding the role of root water uptake in controlling near-surface soil moisture dynamics is essential for hydrologic modeling of water movement in the unsaturated zone and over land surfaces. Root water uptake is commonly accounted for in models of temporal soil moisture dynamics by the addition of a sink term (S) that simulates soil water loss due to vegetation (Molz, 1981). In general, root water uptake by vegetation is a function of plant transpiration, which is dependent on solar radiation absorbed by the plant. For a given time period, the total amount of soil water absorbed by plant roots throughout the root zone is equivalent to the amount of water lost by the plant due to transpiration, which can be expressed as:

$$ET_a = \int_0^L S(z, \mathbf{q}, t) dz \quad (3.1)$$

where ET_a is actual transpiration and L is the rooting depth (Figure 3.1). The value of $S(z, \theta, t)$ has been shown to be dependent on rooting density distribution and soil moisture with depth, which act to distribute atmospheric demand on the plant throughout the root zone (Feddes *et al.*, 1976; Feddes *et al.*, 1978; Perrochet, 1987; Tiktak and Bouten, 1992; Musters and Bouten, 1999). The partitioning of plant transpiration with depth in the root zone determines the role of vegetative on surface saturation dynamics.

Root density with depth throughout the root zone has been assumed to many different distributions for studies involving soil moisture modeling. Estimations of root density distribution with depth are difficult to measure in the field, therefore, empirical relationships that describe local root distribution dynamics for a variety of environments have been proposed for use in modeling uptake of water by plant roots. Feddes *et al.* (1978) suggested a distribution of roots for crop vegetation where root density was constant with depth. A linear decrease in root density with depth has also been used for modeling soil moisture within crop environments (Hoogland *et al.*, 1981; Prasad, 1986), as well as forested ecosystems (Lai and Katul, 2000). An exponential decrease of root density with depth function, which is based on field measurements by Jackson *et al.* (1996) of root density within a variety of biomes, has been recently developed and used for modeling soil moisture in forested environments (Musters and Bouten, 1999; Musters *et al.*, 2000). Extensive root data collected by Jackson *et al.* (1996) show an exponential decrease of cumulative root density with depth for the vegetation types considered (crop, shrub, forest, desert, grassland, and tundra). Jackson *et al.* (1996) also noted considerable variation of cumulative root density in the surface zone (top 10 cm) for different vegetation types. On average, grasses have 39% of roots within the surface zone, trees have 26%, and shrubs have 20% of roots within the surface zone (assuming the same rooting depth for each vegetation type) (Jackson *et al.*, 1996). In light of recent root density data, different vegetation types should have different affects on surface saturation dynamics within the same environment, although this notion has yet to be explored. The field-tested exponential root density distribution affords the opportunity to numerically

explore root density affects on surface saturation with realistic root density distributions for various vegetation types.

Surface saturation is affected by soil characteristics such as surface soil texture and soil layering throughout the root zone. Within the root zone in forested environments, the surface organic litter layer that can accumulate plays an important role in controlling surface soil moisture dynamics. Through modeling analysis, Schaap *et al* (1997) showed that root water uptake within the litter layer of a Douglas fir stand was 2% of total transpiration for a 5 cm thick litter layer (evaporation-dominated litter layer water loss), with 25% of daily litter layer water loss being replenished by capillary rise from the underlying mineral soil. Tobon Marin *et al.* (2000) demonstrated that root water uptake in litter layers extending from 4 cm to 16 cm depth ranged from 15% to 28% of total transpiration. Although previous studies have dealt with controls on soil moisture dynamics within the organic litter layer, the overall role of the litter layer in controlling the temporal dynamics of soil saturation requires further consideration. A better understanding of the role of the organic layer in controlling saturation dynamics can significantly contribute to the prediction of run-off generation and solute delivery from forested catchments to adjacent ecosystems.

The goal of this project was to determine the joint control of soil texture and root density distribution on soil saturation dynamics in a forested environment with low topographic relief. Specifically, this project was designed to: 1) examine the effect of the organic litter layer on mediating surface saturation dynamics in a forested ecosystem, and 2) evaluate the effects of root density distribution dynamics on the control of soil saturation and total root water uptake with varying soil textural properties. A validated

model that incorporates root water uptake in soil moisture evolution was used to first determine the role of the organic layer in controlling soil moisture. Modeling analysis was then used to determine how soil texture and root density distribution interact to control the temporal dynamics of soil saturation in forested environments dominated by vertical soil water movement.

3.2 METHODS

3.2.1 Model Formulation

The purpose of the modeling effort presented in this study was to explore impacts to the frequency of surface saturation dynamics for a range of environments by building on accepted concepts of root water uptake and soil water movement and root water uptake dynamics. The model framework utilized a novel methodology for determining the degree of infiltration after precipitation based on accepted concepts of unsaturated flow. Previously published formulations of the constituents of root water uptake (i.e., Musters and Bouten, 1999; Lai and Katul, 2000) were modified and combined to devise a model with a root water uptake formulation that is simple, yet robust, and applicable to a wide range of soil texture/vegetation type scenarios.

3.2.1.1 Soil Water Movement

To predict temporal soil moisture evolution and soil saturation dynamics in a forested environment, a 1-D form of Richard's equation that includes a sink term was implemented. The form of Richard's equation used can be expressed as:

$$\frac{\partial \mathbf{q}}{\partial t} = \frac{\partial}{\partial z} \left[K(\mathbf{q}) \frac{\partial \Psi}{\partial z} - K(\mathbf{q}) \right] - S(\mathbf{q}) \quad (3.2)$$

where θ is volumetric soil moisture content, K is hydraulic conductivity, Ψ is soil matric potential, and S is the root water uptake term. Values of Ψ and K are functions of θ and were determined by

$$\Psi = \Psi_s \left(\frac{q}{q_s} \right)^{-b} \quad (3.3)$$

$$K = K_s \left(\frac{q}{q_s} \right)^{2b+3} \quad (3.4)$$

where Ψ_s is the saturated matric potential, K_s is the saturated hydraulic conductivity, θ_s is saturated soil moisture, and b is an empirical parameter (Clapp and Hornberger, 1978).

The solution to Richard's equation used in this study was based on a solution derived by George Hornberger at the University of Virginia. Numerical modeling of soil moisture dynamics by means of the Richard's equation was accomplished using a predictor-corrector method. To implement the predictor-corrector technique, the soil moisture equation was modified to:

$$\frac{\partial^2 q}{\partial z^2} = \frac{1}{y} \frac{\partial q}{\partial t} - \left[u \frac{\partial q}{\partial z} - w \right] \frac{\partial q}{\partial z} + S \frac{1}{y} \quad (3.5)$$

where y , u , and w are nonlinear functions of θ given by the equations;

$$y = K \frac{\partial \Psi}{\partial q} \quad (3.6)$$

$$u = \frac{\partial K}{\partial q} \frac{\partial \Psi}{\partial q} + K \frac{\partial^2 \Psi}{\partial q^2} \quad (3.7)$$

$$w = \frac{\partial K}{\partial q} \quad (3.8)$$

The predictor used in the model formulation is an implicit approximation, predicting soil moisture at a node for a time step of $1/2(dt)$ by approximating y , u , and w at the current

time step. The corrector is a Crank-Nicholson approximation that predicts soil moisture evolution at a node for a full time step by using the results from the predictor to get linear expressions of y , u , and w (Remson et al., 1971).

3.2.1.2 Sink Term Formulation

The root water uptake expression used in the model formulation distributes the potential transpiration (ET_p) throughout the root zone by means of a root density function ($g(z)$) and a root water uptake efficiency function ($\alpha(\theta)$):

$$S(z, \mathbf{q}, t) = g(z)\mathbf{a}(\mathbf{q})ET_p(t) \quad (3.9)$$

The expression used for root water uptake is a widely utilized formulation developed by Feddes (1971) and has been shown to be appropriate for a variety of environments, including pine forest ecosystems (Bouten *et al.*, 1992; Musters and Bouten, 1999; Lai and Katul, 2000).

3.2.1.2.1 Root Density Distribution

The root density distribution used for this study is a variation on a root density distribution function resulting from intensive root density measurements within a pine forest ecosystem. Musters and Bouten (1999) determined that pine root density in an Austrian pine forest exhibits a power law decrease with depth, which can be expressed by the function:

$$Y(z) = Y(0) \times \left[1 - (z/L)^a \right] \quad (3.10)$$

where z is depth (cm), L is maximum rooting depth (cm), the exponent a is an empirical coefficient that distributes root density with depth, and $Y(0)$ is the root density at the soil

surface (cm cm^{-3}). For the root density function to be appropriate for model use, root density at each depth must be expressed in relation to total root density throughout the root zone. To generalize the root density function and to make the function dimensionally correct for model input, root density at depth is normalized by the total root density throughout the root zone by the expression;

$$g(z) = \frac{1 - (z/L)^a}{\int_0^L 1 - (z/L)^a dz} \quad (3.11)$$

in which $g(z)$ has the appropriate dimensions of cm^{-1} (Figure 3.2). The modified form of the Musters and Bouten (1999) expression for root density distribution is similar in shape to the root density distribution described by the intensive, multi-biome field study of Jackson, *et al* (1996), furthering the notion of the realistic nature and the range of the root density distribution devised for this study.

3.2.1.2.2 Root Efficiency Function

The efficiency in which roots will uptake water throughout the root zone is a function of the ratio of soil moisture at the local depth to saturated soil moisture content (Herkelrath *et al*, 1977). For this study, the efficiency of root water uptake throughout the root zone was determined by a maximum efficiency term (Tiktak and Bouten, 1992) and a reduction term (Lai and Katul, 2000):

$$\mathbf{a}(\mathbf{q}) = \left(\frac{\mathbf{q}}{\mathbf{q}_s} \right) \left(\frac{\mathbf{q} - \mathbf{q}_w}{\mathbf{q}_s - \mathbf{q}_w} \right)^{\frac{\gamma}{\mathbf{q} - \mathbf{q}_w}} \quad (3.12)$$

where θ_s is saturated soil moisture content, θ_w is the wilting point soil moisture and the γ term is an empirical constant. Wilting point soil moisture was derived from a common

estimate of the wilting point matric potential (-15000 cm) (Feddes *et al.*, 1976) and the Clapp and Hornberger (1978) relationship between Ψ and θ .

The maximum efficiency term (saturation fraction) describes how efficiently roots will uptake water when not limited by water availability. The reduction function is applied to the uptake term to determine actual water uptake under conditions when soil moisture availability is limiting root water uptake (Figure 3.3). Specifically, the reduction function used here that was formulated by Lai and Katul (2000) was derived from the empirical relationship between ET_p/ET_a and Ψ put forth by Feddes *et al.* (1976). The reduction function essentially determines the rate at which roots will shut down water uptake. As θ approaches θ_w , the reduction function approaches 0 and as θ approaches θ_s , the reduction function goes to 1. The rate at which the reduction function changes with soil moisture is a function of the exponent γ (Lai and Katul, 2000). A value of 0.003 for γ was used in this study which insured that the shape of the reduction function matched the shape of a reduction function derived by Tiktak and Bouten (1992), which is a more robust function that has been applied in numerous studies (Bouten *et al.*, 1992; Bouten and Witter, 1992; Musters and Bouten, 1999; Musters *et al.*, 2000) yet does not have the ease of implementation of the Lai and Katul (2000) version of the reduction function used in this study.

3.2.1.3 Model Boundary Conditions

Boundary conditions implemented within the model framework were:

1. No bare soil evaporation at the soil surface (potential transpiration is equal to measured potential evapotranspiration) due to dense vegetation cover.

2. The bottom of the soil domain was at the water table.
3. Precipitation input into the soil domain was expressed as a condition of the matric potential gradient at the soil surface. Precipitation rate was input as the maximum water flux into the soil surface (using a Darcian flux) and the matric potential at the soil surface that satisfied this input condition was calculated. Soil water movement into the soil domain was calculated by the expression:

$$q = -K_2 \left(\frac{d\Psi}{dz} \right) + K_2 \quad (3.13)$$

where q is the precipitation rate and the subscript represents the node location. With the hydraulic variable information from the previous time step, the matric potential at the soil surface was calculated by the expression:

$$\Psi_1^j = \Psi_2^{j-1} - \left[\frac{q^j - K_2^{j-1}}{-K_2^{j-1}} \right] dz \quad (3.14)$$

where the superscript j represents the model time step. For conditions when the value for Ψ_1 was greater than Ψ_s at the top node, the matric potential gradient was such that the ground could not absorb all the precipitation so Ψ_1 was set equal to Ψ_s at the top node. Matric potential at the top node was then converted to a value of soil moisture (by means of the Ψ - θ relationship of Clapp and Hornberger(1978)) and input into the model to represent the precipitation effect on soil moisture.

3.2.2 Field Experiment

3.2.2.1 Study Site

Field data were collected in a forested stand at the upland fringe of a tidal salt marsh located within the Virginia Coastal Reserve (VCR/LTER) site on the Eastern Shore of

Virginia. Vegetation at the site is predominantly Loblolly pine (*P. taeda*) mixed with red cedar (*J. virginiana*). Loblolly pine and red cedar DBH (diameter at breast height) at the upland site is on the order of 40 cm and 20 cm, respectively. Site meteorological and hydrologic variables for model were measured from July 14-August 12, 1999. This section is intended to give an overview of the field site and data collection and analysis techniques. A more complete description of methodology is given in the second chapter of this thesis.

3.2.2.2 Hydrologic Measurements

Near-surface soil moisture was measured in the upland forest fringe using a time domain reflectometry (TDR) probe (Campbell Scientific CS615). The 30 cm long probe measured wave period within the upper root zone every hour during the summer of 1999. Hourly measurements of wave period were recorded by a Campbell Scientific 21X data logger. Wave period output was converted to soil moisture by a calibration curve of wave period and measured volumetric soil moisture (Appendix A). The hourly time step for measuring soil moisture insured that rain events during the study period could be captured by the probe while keeping the number of moisture measurements at field capacity to a minimum for accurate representation of field conditions.

The depth to the water table at the study location was measured daily during low tide at a well that was adjacent to the soil moisture probe. Low tide water table elevation was considered an accurate representation of daily water table although the water table elevation at the study site varied on a tidal cycle time scale due to tidal forcing (see Chapter 2). Low tide water table elevation ranged from 0.3 m-0.8 m above MSL, or 0.7

m - 1.2 m below the ground surface. Average measured water table depth during the study period was on the order of 1.0 m below the ground surface.

3.2.2.3 Meteorological Measurements

Micrometeorological variables needed for model inputs were measured within the upland fringe and in the adjacent tidal salt marsh. Precipitation was measured every hour with a tipping bucket (Campbell Scientific TE525) approximately 100 m from the study site at an LTER micrometeorological station located within the marsh. Values of photosynthetically active radiation [PAR] (Li-Cor 190S) and air temperature (Campbell Scientific HMP35C) needed for potential transpiration calculations were measured at the marsh micrometeorological station, while soil heat flux (Campbell Scientific HFT) was measured within the upland fringe. Hourly measurements taken in the marsh and in the upland fringe were recorded on a Campbell Scientific 21X datalogger.. Potential transpiration was then calculated by means of the Priestly-Taylor (1972) formulation for latent heat flux under the assumption that there was no bare soil evaporation and all potential evapotranspiration calculated from the Priestly-Taylor formulation was considered equal to potential transpiration.

3.2.2.4 Soil Properties

Soil type was determined by calculating the sand, silt, and clay fraction of soil samples that were extracted to a depth of 1.2 m. The surface soil at the upland fringe is comprised of an organic litter layer that is approximately 0.12 m thick. Below the litter layer is a loam layer that extends to a depth of 0.80 m and a basal sandy loam soil layer

below 0.80 m depth. Values of soil textural properties with depth and the associated soil hydraulic properties are given in [Table 2.1](#) (70 meters from the creek bank). The values of θ_s , K_s , and b for the loam and sandy loam layers were calculated by the Saxton *et al* (1986) pedotransfer functions given in chapter 2. The θ_s and K_s values for the litter layer were taken from a study by Musters and Bouten (1999) in which hydraulic variables were measured *in situ* on a pine forest floor. The litter layer b value is an approximation derived from a study by Katul *et al* (1997) which showed that macropores in the near-surface root zone cause lowered values of the empirical b coefficient than b values in the lower root zone. Litter layer Ψ_s is an estimation based on the assumption that the porous nature of the litter layer will make the litter layer Ψ_s significantly less than Ψ_s for the underlying loam layer (Schaap *et al*, 1997).

Rooting depth at the field site was estimated using previous studies of pine root depth in layered sandy soils and pine root depth in an environment with a fluctuating water table. Pine roots in a sandy soil environment have been shown to cease vertical expansion at the contact between a lower permeability surface soil layer and a higher permeability soil layer at depth (Musters and Bouten, 1999). Furthermore, a fluctuating water table causes pine rooting systems to be fairly shallow with respect to vertical development, with the taproot extent remaining low due to anoxic conditions associated with high water table elevations (White *et al.*, 1971). Therefore, the root depth for the field site is assumed the same as the depth of the contact between the loam and sandy loam soil layers.

3.3 RESULTS AND DISCUSSION

3.3.1 Overview

In this section, measured depth-averaged near-surface (top 30 cm) soil moisture is compared to modeled soil moisture for model validation. The role of the organic litter layer in controlling near-surface saturation dynamics is examined by comparing the ratio of modeled surface soil moisture to saturated moisture content for soil conditions with and without a surface organic layer present. The effect of root density distribution with depth on near-surface soil saturation is analyzed through modeling the amount of time that surface (top 10 cm) soil moisture is at least $0.8\theta_s$ (an arbitrary saturation threshold) for soils with varying texture and root density distributions that represent different vegetation types. Total root water uptake throughout the root zone for model simulations of soil moisture for varying root density and soil texture is discussed in the context of the variability of root water uptake as a function of vegetation type.

3.3.2 Model Validation Results

3.3.2.1 Model Parameterization

Input variables used for model validation were derived from direct field measurements and literature values based on field conditions similar to those at the study site. The empirical a variable used for root density was 0.4, which is a root extinction value specific to pine roots (Musters and Bouten, 1999). Water table depth input into the model was 0.95 m (average water table depth for the study period). Rooting depth was 0.8 m, which is consistent with the depth of the contact between soil layers. The initial soil moisture distribution with depth input into the model was determined by field

measurements of matric potential on day 194 at depths of 25 cm, 45 cm, 75 cm, and 105 cm. A polynomial interpolated was used to get initial matric potential at each node (1 cm spacing) from values of measured initial matric potential at the four depths in the soil column. Initial soil moisture at each node was then obtained by using the Clapp and Hornberger (1978) relationship between soil moisture and matric potential. Measured values of precipitation and potential transpiration during the field campaign were used as model inputs (Figure 2.4)

3.3.2.2 Near-Surface Soil Moisture

Comparison of model results of near-surface soil moisture (top 30 cm) to field measurements during the 29-day study period (days 195-223) in the summer of 1999 shows that the model captures the soil moisture dynamics both during rain events and during periods of drying where the soil water content approaches field capacity (Figure 3.4). Model results of soil moisture agree reasonably well with the overall measured trend of near-surface soil moisture conditions after drainage has occurred following precipitation. The diurnal amplitude of soil moisture due to root water uptake during the day and soil moisture recharging at night is well predicted. Agreement between measured and modeled soil drainage and variation in daily near-surface soil moisture during drying periods suggests the validity of root water uptake determined by the model and the validity of hydraulic variables used as model inputs derived from pedotransfer functions. Root mean square error (RMSE) for the measured and modeled time series of near-surface soil moisture for the study period is 0.007.

During rain events and periods directly following rain events, the predicted soil moisture over the top 30 cm shows the greatest deviation from the measured soil moisture (Figure 3.4). On day 220, the initial rise of soil moisture due to the onset of a precipitation event is similar between measurements and modeled results. When precipitation begins to infiltrate, the modeled near-surface soil moisture shows more rapid drainage than measured soil moisture values. The model assumes that all water not infiltrated is run-off, thereby not accounting for ponding of water on the soil surface during rain events. The maximum difference between measured and modeled soil moisture in the top 30 cm is 1.7% volumetric soil moisture during the drying period after the day 220 rain event, therefore the model parameterization is deemed adequate to predict soil moisture dynamics during drying periods as well as directly following precipitation events.

Figure 3.5 shows the separation of modeled soil moisture in the top 30 cm into depth-averaged soil moisture in the surface litter layer (0-12 cm depth) for the simulation period and depth-averaged soil moisture in the loam below the litter layer (13-30 cm depth). During periods between rain events, soil moisture for the organic layer is maintained at a field capacity of 16% and soil moisture for the underlying loam layer has a field capacity of 23% volumetric soil moisture content. During rain events, the modeled soil moisture for the organic layer increases significantly with no increase in depth-averaged soil moisture for the loam. The precipitation on day 195 caused elevated soil moisture content throughout the top 30 cm of soil due to storm duration, however precipitation on day 203 increased soil moisture in the organic layer from 17% to 33% with only a 2% volumetric soil moisture increase in the loam. Precipitation on days 205 and 220 caused

an 8% volumetric soil moisture increase in the organic layer with no associated increase in soil moisture in the underlying loam soil. Increases in organic layer soil moisture during storm events corresponding to a low degree of variation in soil moisture below the organic layer is mediated by organic layer thickness, differences in hydraulic properties between the soil types, and variation in root water uptake dynamics between the soil layers (discussed in the next subsection). Low soil moisture content at field capacity and the 'flashy' nature of the organic layer response to precipitation events gives an indication of the role that the organic litter layer plays in mediating depth-averaged near-surface soil moisture dynamics in forested ecosystems. The role of the organic litter layer in controlling near-surface saturation is discussed later in this chapter.

3.3.2.3 Root Water Uptake

The modeled uptake of water throughout the entire root zone (80 cm depth) for the study period is compared to measured potential evapotranspiration in [Figure 3.6](#). For the summer study period, the potential amount of water that could have been lost due to evapotranspiration was 25.9 cm. The plants within the upland fringe were transpiring well below potential during the study period, taking up 13.9 cm of water, or 54% of potential water loss. The ratio of plant water uptake to potential uptake measured in this study is similar to values given by Lai and Katul (2000) for a pine-dominated forest ecosystem. This study, however, was conducted in a more mesic environment than the study by Lai and Katul (2000), with roots extending to within 15 cm of the average water table depth and higher average values of near-surface soil moisture. Low average root water uptake, in comparison to potential, within the study environment was facilitated by

low root density in the regions of soil with the highest average values of soil moisture. In general, higher average soil moisture content at depth did not compensate for the exponential decrease in root density with depth to keep the vegetation transpiring at potential.

Distribution of root water uptake throughout the root zone illustrates the control of the interaction between uptake efficiency and root density dynamics on total plant water uptake dynamics (Figure 3.7). On a local scale, the rate of root water uptake was greatest during the study period in the organic litter layer (top 12 cm). Water uptake in the near-surface zone (top 30 cm) is further facilitated by the replenishment of water lost to evapotranspiration from deeper in the root zone. Root water uptake in the loam below the organic layer also remains constant during the study period, although uptake does decrease with depth. The consistent root water uptake within the organic layer and the loam layer was facilitated by the low degree of soil moisture variability during the study period. Soil moisture within the organic layer ranges from 16% to 33% volumetric soil moisture, however the storm-induced peak soil moisture values are dissipated within hours of the storm event, with no appreciable effect on root uptake dynamics in the organic layer. The soil moisture distribution with depth in the organic layer causes consistent root uptake efficiency with depth, thereby resulting in a fairly constant value of root water uptake with depth. In the underlying loam, the efficiency value is also constant (due to an even lower degree of variability in soil moisture as given by Figure 3.5), yet is a lower average value than in the organic layer. Differences in efficiency function values between the two layers is driven by soil moisture and hydraulic properties specific to each soil and causes the sharp contrast between uptake values for both layers,

with root density distribution driving the decrease in root water uptake with depth. Approximately 38% of the total roots were within the organic layer at the upland fringe. For the entire study period, 29% of the total root water uptake was in the organic litter layer and 71% was in the underlying loam layer. These results are similar to those of Tobon Marin (2000), who reported a value of 28% total water uptake in the organic layer (16 cm thickness) of a sedimentary plain in Amazonia where average organic layer soil moisture was approximately 10%.

The importance of the organic litter layer in controlling root water uptake and soil moisture dynamics in forested environments is apparent from the model validation simulation. The organic litter layer can be crucial in determining infiltration dynamics and root water uptake rates. Next, the relative importance of the organic litter layer in controlling soil saturation dynamics in the near-surface zone (top 30 cm) is investigated numerically by examining soil moisture dynamics with and without a surface organic litter layer.

3.3.3 Organic Layer Control of Surface Saturation Dynamics

3.3.3.1 Modeling Analysis

The role that the surface organic layer has in mediating surface saturation conditions in a forested environment was explored numerically using a two-layered soil domain (organic layer above loam) and a single layer soil domain (loam). Soil moisture dynamics were modeled in the two soil domains using the Richard's equation model with sink term. Model simulation time, hydraulic properties for the soils considered, rooting depth for the model simulations, atmospheric inputs, and boundary conditions were the

same as those used as model inputs for the model validation simulation. The water table was set at a depth of 1 m for this modeling analysis and the initial matric potential gradient for all simulations was set at a hydrostatic condition (matric potential [in |cm|] is equal distance above the water table). The loam extended to a depth of 100 cm for the single layer soil domain. For the two-layered soil domain, the organic layer extended from 0-12 cm depth, with the loam extending from 13-100 cm depth.

Depth-averaged soil saturation dynamics for the top 30 cm of soil, expressed as a ratio of soil moisture to saturated soil moisture (S_r) for both soil domains and the differences between S_r for the simulation period for both soil domains is given in [Figure 3.8](#). For the two-layer system, depth-averaged soil moisture in the top 30 cm ranged from $.55\theta_s$ to $.72\theta_s$. Depth-averaged soil moisture for the single-soil simulation (loam only) ranged from $.62\theta_s$ to $.92\theta_s$. The percent difference between depth-averaged surface soil moisture for the two simulations is approximately 15% during field capacity conditions and ranges from 30% to 38% during precipitation events. Total root water uptake during the model simulation in the top 30 cm for the two-layer simulation was 9.1 cm (35% of cumulative ET_p), while total root water uptake for the single-soil simulation was 11.9 cm (46% of cumulative ET_p).

At the onset of precipitation, the percent difference between S_r for both simulations decreases rapidly due high infiltration capacity of the porous organic layer. The surface organic layer infiltrates water faster than the surface loam, thereby causing the depth-averaged surface soil moisture for the two-layered system to become closer to the depth-averaged surface soil moisture for single soil domain until the loam starts to infiltrate the precipitation. The decrease of S_r after precipitation events is more significant in the two-

layered system due to differences in saturated hydraulic properties between the organic layer and the loam. Saturated hydraulic conductivity for the organic layer, taken from Musters and Bouten (1999) was 0.069 cm/min and saturated hydraulic conductivity for the loam, determined by the pedotransfer function of Saxton *et al* (1986), was 0.031 cm/min. The factor of 2 difference in saturated hydraulic conductivity between the two soils caused the difference in drainage dynamics between the two model simulations. The lower K_s for the loam in comparison to the K_s for the organic layer facilitated the increased root water uptake for the single-soil simulation due to higher water of the loam over the organic litter layer. In general, the porous nature of the organic layer causes a low degree of surface saturation after precipitation events through fast drainage and a low degree of surface saturation at the onset of precipitation events due to low field capacity soil moisture.

Soil texture plays an important role in determining soil saturation dynamics by controlling soil water drainage dynamics. Along with soil textural properties, rooting dynamics are also key factors in determining the temporal dynamics of soil saturation. The distribution of root density with depth contributes to the partitioning of root water uptake, which in turn affects soil moisture content throughout the soil column and soil saturation dynamics at the soil surface following precipitation events. The next section examines the combination of soil texture and root density controlling saturation dynamics and root water uptake for a variety of soil textures and root density distributions with depth.

3.3.4 Soil Texture and Root Density Distribution Control on Surface Saturation

3.3.4.1 Model Parameterization

To model the effects of soil texture and root density on near-surface saturation dynamics, model simulations were run with soil textures of increasing clay/decreasing sand content and root density distributions that decreased in the percent of total roots in the surface soil zone (top 10 cm of soil). For this analysis, soil moisture within the top 10 cm are considered to be important for mediating run-off generation in regions with low topographic influence on soil saturation dynamics. Soil textures used in the modeling analysis were devised to represent end-member sand and clay textures as well as a range of loam textural conditions. Textural scenarios considered decreased linearly in percent sand from 90% to 10% while increasing linearly in percent clay from 10% to 53.8% (see [Table 3.1](#)). Values of θ_s , K_s , and b , used as model input variables, for each soil texture used in model simulations were derived from the Saxton *et al* (1986) pedotransfer functions, while Ψ_s values were taken from Clapp and Hornberger (1978). Root density distribution with depth was determined for each model simulation by changing the root density exponent (a) in [equation 3.11](#). The root density exponent controls the shape of the root density distribution with depth, thereby controlling the fraction of roots within the surface zone ([Figure 3.9](#)). Root density exponent values used ranged from 0.1 to 10, which relates to a power law decrease in associated cumulative root density in the top 10 cm of soil (R_{10}) from 43% to 15% ([Figure 3.10](#)).

Model runtime for each model simulation was 29 days, with measured time series of precipitation and potential evaporation from the field experiment used as model inputs. Similar to the model simulations with and without an organic layer, water table depth was

1 m below the ground surface and hydrostatic initial conditions were assumed. Model outputs for each combination of texture and root density included the total time that the surface soil layer was close to saturation ($\geq 0.8\theta_s$) and the total amount of water uptake as a function of potential transpiration. The role that root density distribution with depth has on determining the surface saturation and root water uptake dynamics for varying soil textures is discussed next.

3.3.4.2 Model Results

The amount of simulation time that the surface layer (top 10 cm) was close to saturation ($\geq 0.8\theta_s$) and total root uptake for each combination of soil texture and root density are given by the plots in [Figure 3.11](#). In general, low clay content/high sand content values kept the surface soil dry for all values of the root density exponent due to the low storage capacity of these sandy soils. As clay content increased linearly from 10% to 41.3%, the percent of the total time that the surface was close to saturation (T_s) increased from 0 to 100 for all root density exponent values, with soil textures with high associated values of root density exponent maintaining an overall higher % saturation time. The maximum value for T_s was reached at a soil texture of 40% sand and 41.3% clay due to the high magnitude of Ψ_s (-63 cm). Beyond the 40% sand/41.3% clay texture, T_s decreased as a function of decreased Ψ_s and increased root density closer to the soil surface. The total root water uptake for the simulations generally increased with an increase in clay content (due to low drainage causing more available water for root uptake) and showed a low degree of variability with an increase in the root density exponent value. Total root water uptake ranged from 70% total ET_p to 90% total ET_p for

all of the model simulations (maximum root water uptake occurred at 40% sand/41.3% clay for all values of the root density exponent). Representative root density exponent values used in this study were chosen to correspond to cumulative top 10 cm root density values of 43% (similar to grass), 20% (similar to trees), and 15% (similar to shrubs). Vegetation types associated with root concentration are taken from results reported by Jackson *et al.* (1996).

The representative plots show that root density did not become important in mediating surface saturation until sand content becomes low enough and clay content becomes high enough to decrease soil drainage (Figure 3.12). It was not until the sand content decreases to 70% and the clay content increased to 22.5% that there was a difference in surface saturation for different rooting types. For clay contents between 22.5% and 41.3%, T_s increased at the lowest rate for the simulations with the 0.1 root density exponent and at the highest rate for the 10 root density exponent simulation, with a similar increase in T_s for the 0.1 and 1 exponent simulations (less than 10% difference). Similarity between the 0.1 and 1 root exponent simulations is a result of the similar shape of the profiles with depth. Even though the percent of roots in the top 10 cm is different between the two root density distributions, the similar distribution of roots with depth for both profiles (below 15 cm) ensured similar root-driven weighting of potential transpiration with depth, causing similar depth-averaged uptake in the drier surface soil for both distributions. The value for T_s when the root density exponent equaled 10 was the greatest for each textural combination because of the high degree of roots with depth (85% below 15 cm). High root density exponent values caused root distribution to be the same at each depth, thereby causing the uptake to occur at depth (where moisture content

is high) because the root term is weighting potential transpiration the same at each depth and the efficiency function is dominating uptake dynamics. When surface soil moisture is high after rain events, the uptake in the surface layer is still low with higher root density exponents because the lack of roots keeps the total uptake low.

High clay content soil textures caused the difference in T_s to increase for the simulations with low root density exponents. Simulations with textural combinations of 30% sand/47.5% clay and 20% sand/53.8% clay show a greater increase in difference of T_s than the for lower clay content simulations because of the increased role of the efficiency term in regulating the distribution of root water uptake with depth. The increased clay content, and associated decreased sand content, caused drainage to decrease in general and soil moisture to be high throughout the soil domain. High soil moisture throughout the soil column caused the efficiency term to be the same with depth, which means that the root density term becomes more important in the distribution of potential transpiration with depth. When soils are wet throughout the soil domain, the difference in density distribution between the lower root density exponents becomes apparent. When there is water available in the top 10 cm, the vegetation with 43% of total roots in the top 10 cm will draw in that water and keep the surface layer drier than the vegetation with 25% of roots in the top 10 cm. The similar shape of the root density with depth for the lower root density exponent values is not a factor for wetter soils because plants are not limited to water uptake at depth.

Total root water uptake for simulations with the representative root density exponent values shows a low degree of variation for simulations run with each soil type, suggesting that total root water uptake does not vary significantly among different vegetation types

within the same soil texture. The grass root density exponent caused the lowest degree of root water uptake due to root concentration near the surface (low average soil moisture), with the shrub root density causing the highest total root water uptake due to a higher relative concentration of roots with depth. However, even though there are these differences in total water uptake between vegetation types at each soil texture, the difference between total water absorbed by plant roots for the 0.1 and 10 root density exponents remains at approximately 5% total ET_p for most of the simulations (1.3 cm difference in water uptake). There is the same total amount of roots for each root density distribution, but distribution of roots with depth causes root water to be taken up preferentially at certain depths. Although soil water may be taken up at different locations in the soil column, the overall average root water uptake is still preserved regardless of vegetation type. An important addendum to this discussion is that, in reality, the wilting point soil moisture (θ_w) may be a function of plant type as well as soil matric potential. Including vegetation influences on θ_w would effect the efficiency of root water uptake for differing vegetation types in the same soil texture. However, since θ_w is usually a fraction of both θ_s and θ with depth, the effect of varying θ_w to include vegetation influences would only be significant under xeric conditions.

3.4 CONCLUSIONS

This study explored the control of soil texture and root density distribution on run-off generating conditions in forested ecosystems with low topography. Specifically, the role of the surface organic litter layer in controlling surface saturation conditions and the control that root density distribution has on controlling surface saturation dynamics for

varying soil textures were examined to further understanding of under what conditions frequent surface saturation can be expected. Numerical analysis of near-surface soil moisture for a loam soil column and a litter layer/loam soil column showed that the litter layer mediates surface saturation by keeping near-surface field capacity soil moisture low during period between storm events while facilitating rapid drainage of soil water directly after storm events.

Modeling of surface saturation dynamics for varying root density distributions and soil textures showed even distribution of roots with depth caused the surface saturation time to be high for all soil textures considered due to the low relative root density in the upper soil. The amount of time that the surface was close to saturation at lower clay content textures was similar for lower root density exponent values due to a combination of dry surface soils causing low uptake of surface roots and similar root density distributions with depth (below 15 cm) causing the same degree of low uptake with depth. For higher clay content textures, the difference in the amount of time that the surface is close to saturation for the lower root density exponent values increases because low drainage cause water to be available to surface roots where root density is the highest, thereby increasing the role of root density in controlling surface saturation dynamics. Total root water uptake during the model simulation periods is greatest for high root density exponents because of the total amount of roots is greatest at depth where average soil moisture is the highest. The low amount of variation between total water uptake for varying root density at the same soil texture suggests that vegetation with the same rooting depth essentially uptake the same amount of water when exposed to the same

conditions, but the water is just taken in preferentially at different locations in the soil column.

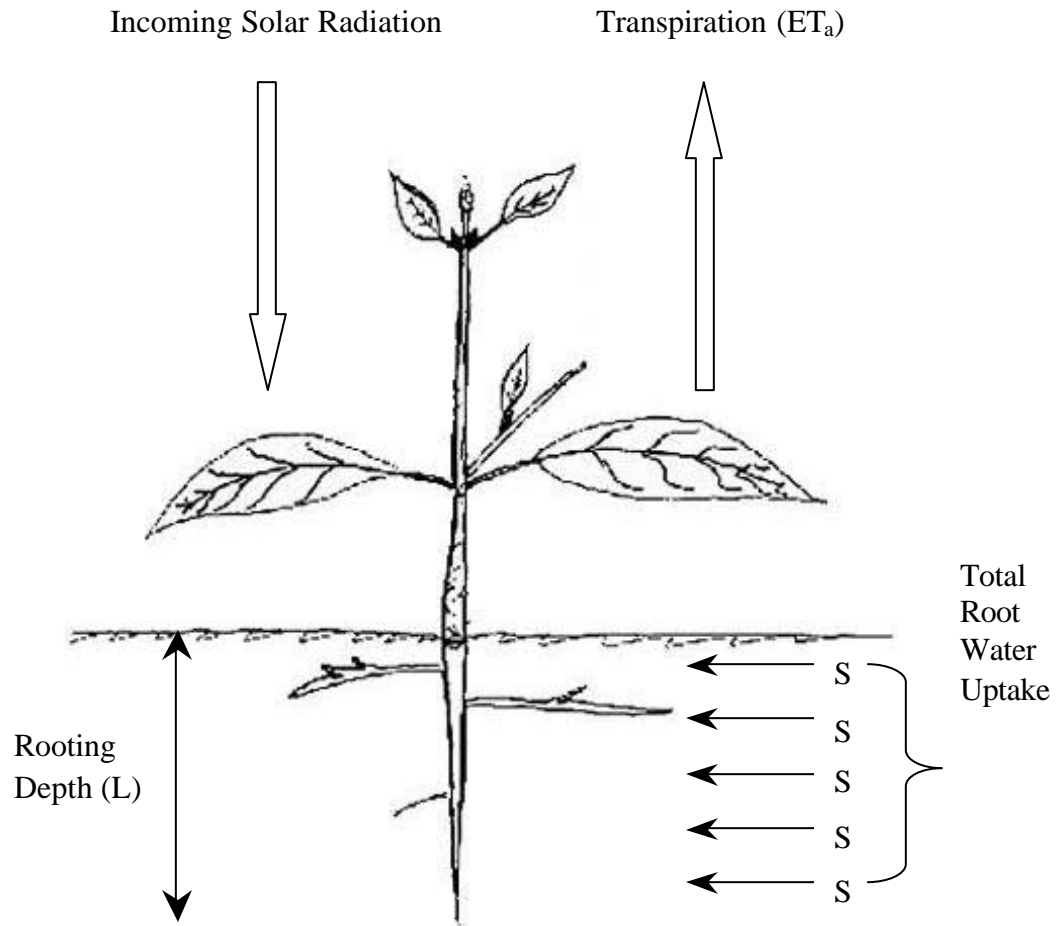


Figure 3.1 Schematic diagram representing the atmospheric demand on vegetation and associated transpiration and root water uptake.

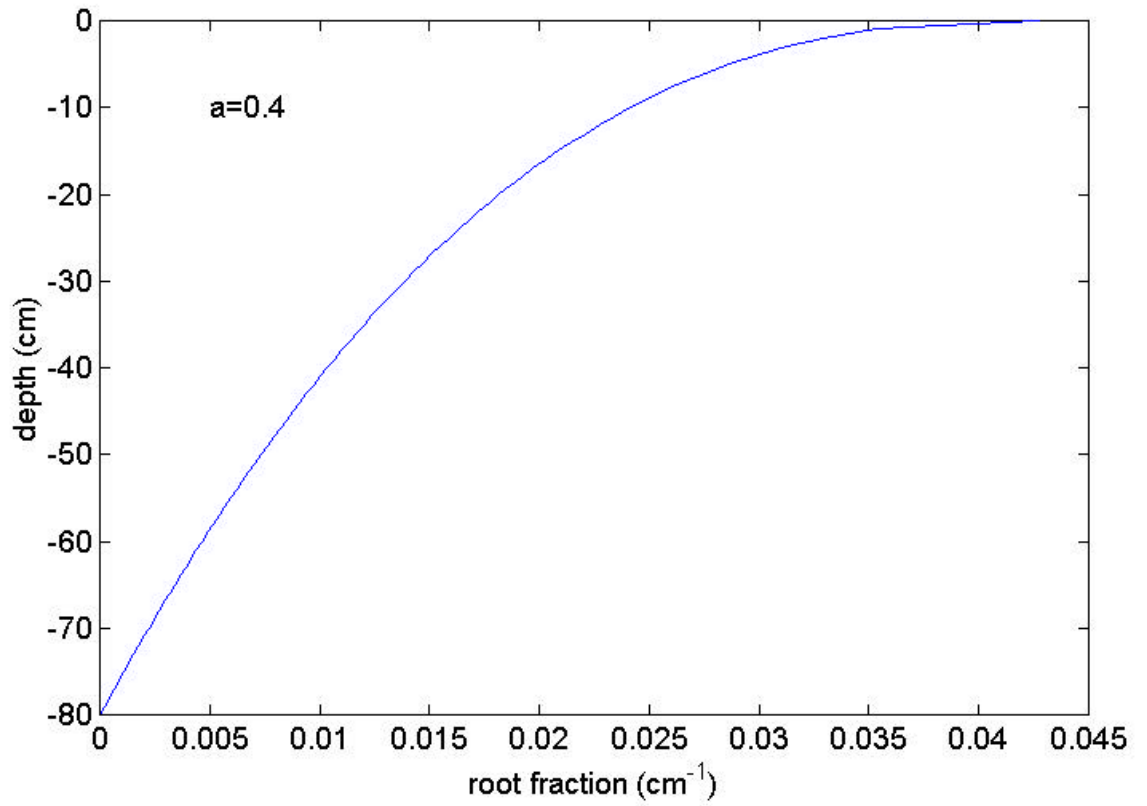


Figure 3.2 Fraction of roots with depth for an empirical exponent (shape variable) of 0.4, as explained by the modified Muster and Bouten (1999) expression for root density distribution.

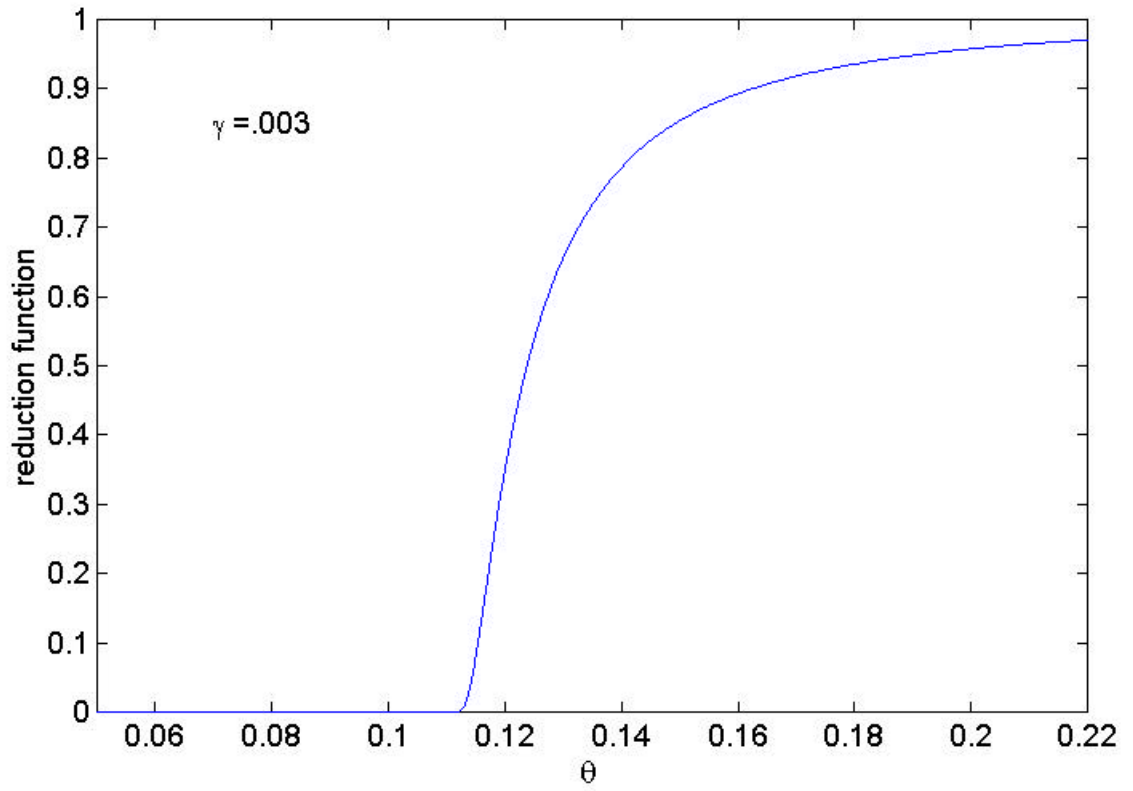


Figure 3.3 Root efficiency reduction term for a range of soil moisture values with an empirical exponent of 0.003, indicative of a loam.

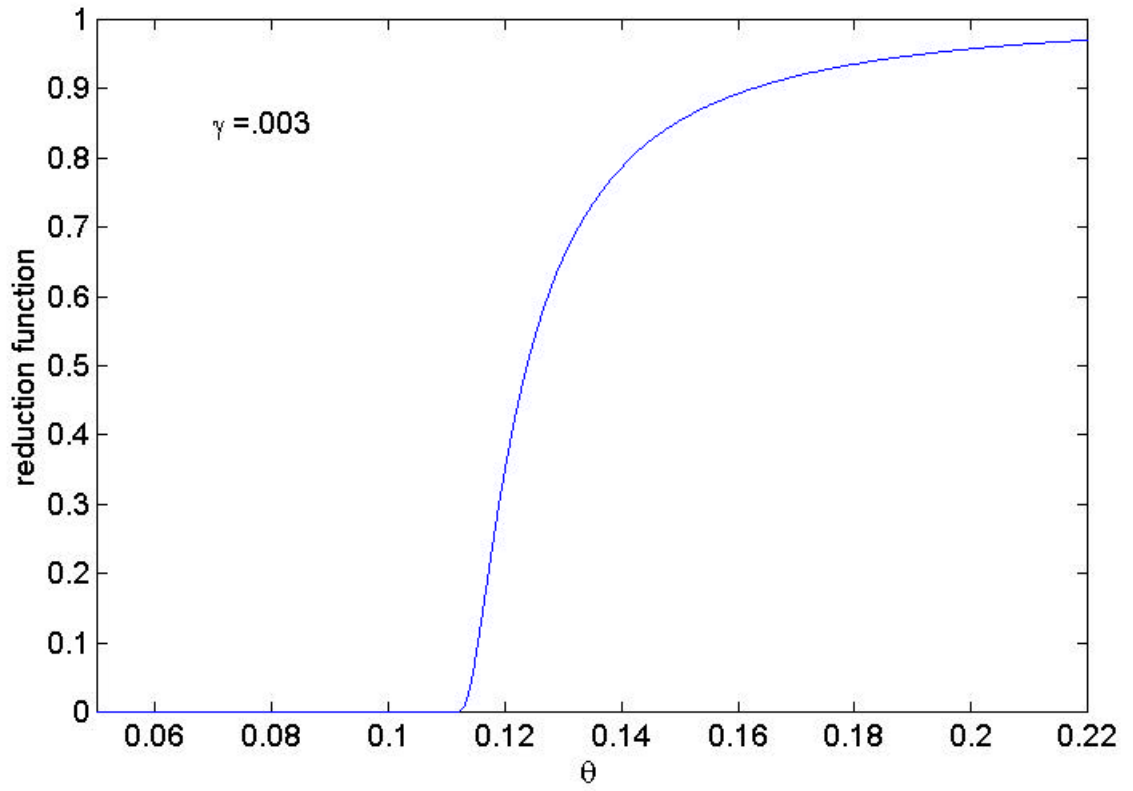


Figure 3.3 Root efficiency reduction term for a range of soil moisture values with an empirical exponent of 0.003, indicative of a loam.

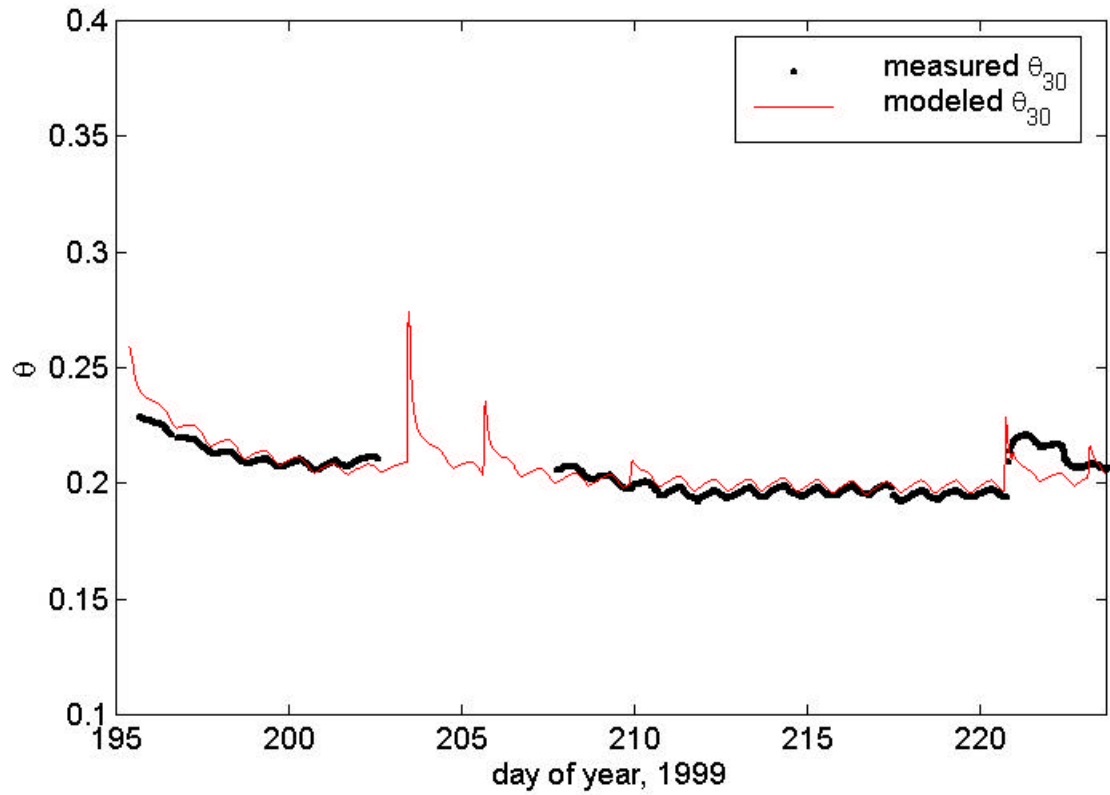


Figure 3.4 Measured and modeled depth-averaged soil moisture for the top 30 cm of soil (θ_{30}) at the study site for the 30 day model simulation period. The lack of measured soil moisture from days 202-207 was due to instrument error.

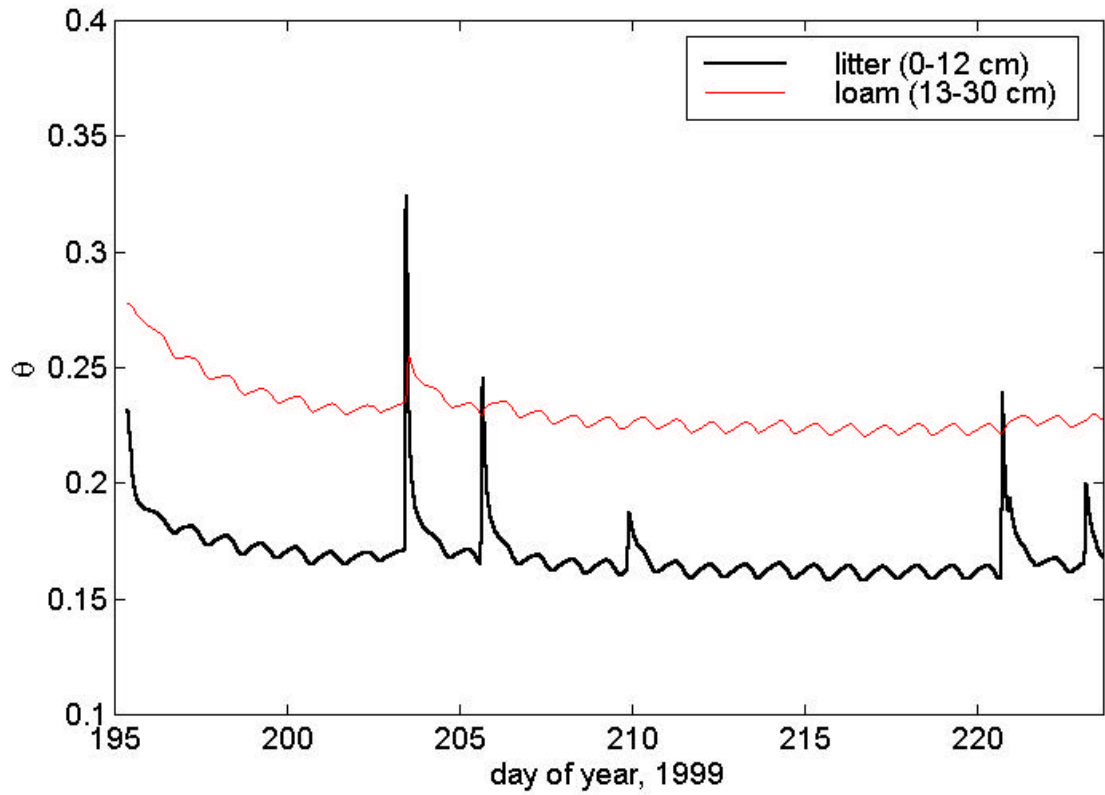


Figure 3.5 Depth-averaged modeled volumetric soil moisture (θ) at the study site for the organic litter layer (0-12 cm depth) and the underlying loam layer (13-30 cm depth).

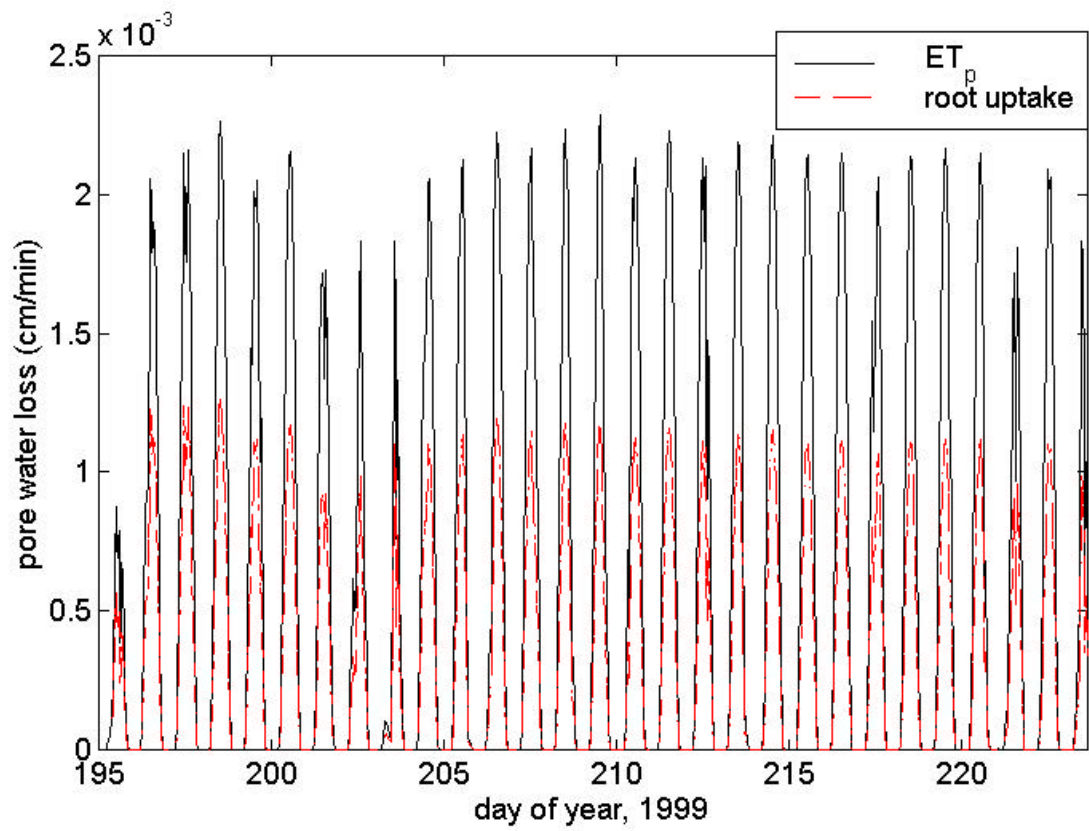


Figure 3.6 Measured potential evapotranspiration (ET_p) and modeled root water uptake for the 30-day model simulation period.

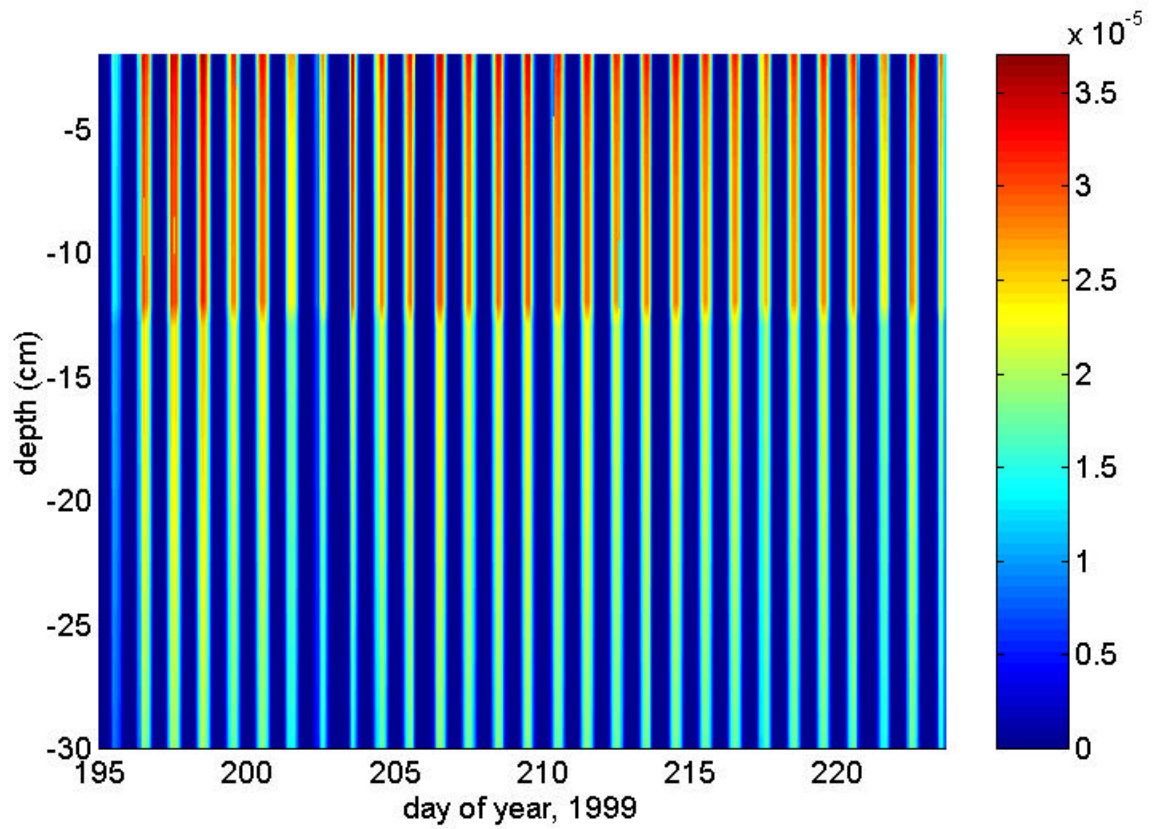


Figure 3.7 Contour plot of the time series of modeled root water uptake with depth at the study site during the 30-day simulation period.

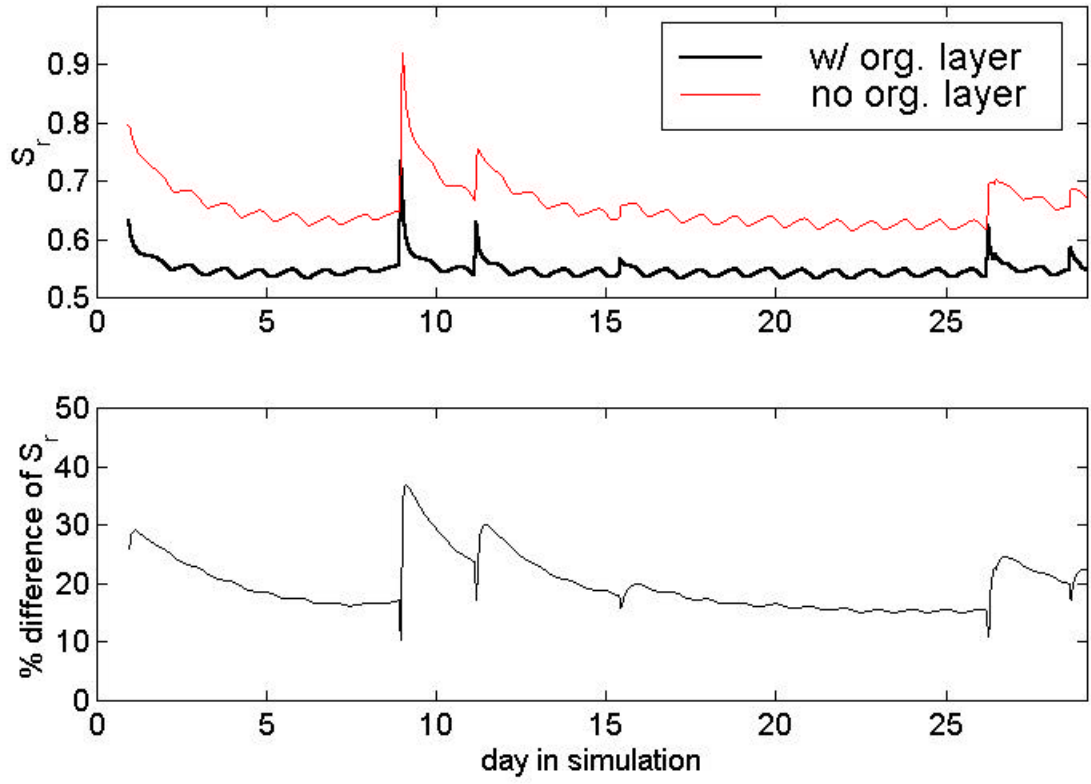


Figure 3.8 The ratio of depth-averaged θ for the top 30 cm to θ_s (S_r) and the difference in S_r for model simulations with and without a organic litter layer.

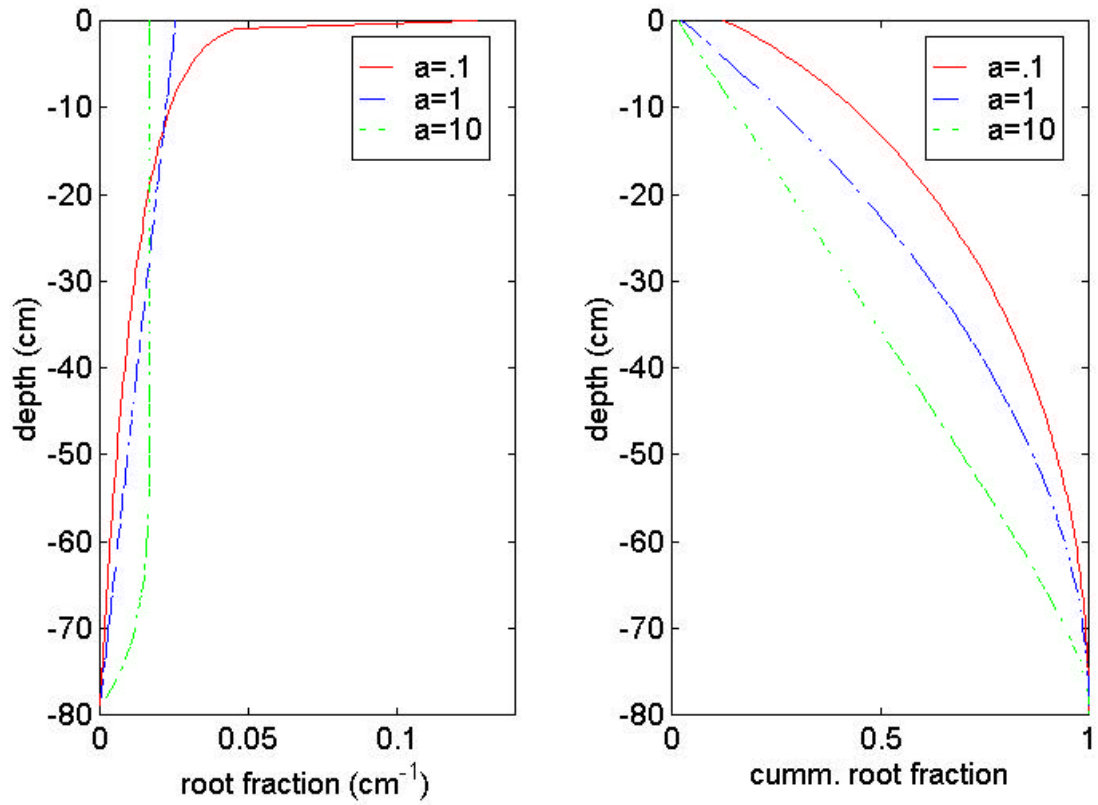


Figure 3.9 Root fraction and cumulative root fraction with depth for a three order of magnitude variation in the root shape factor (a).

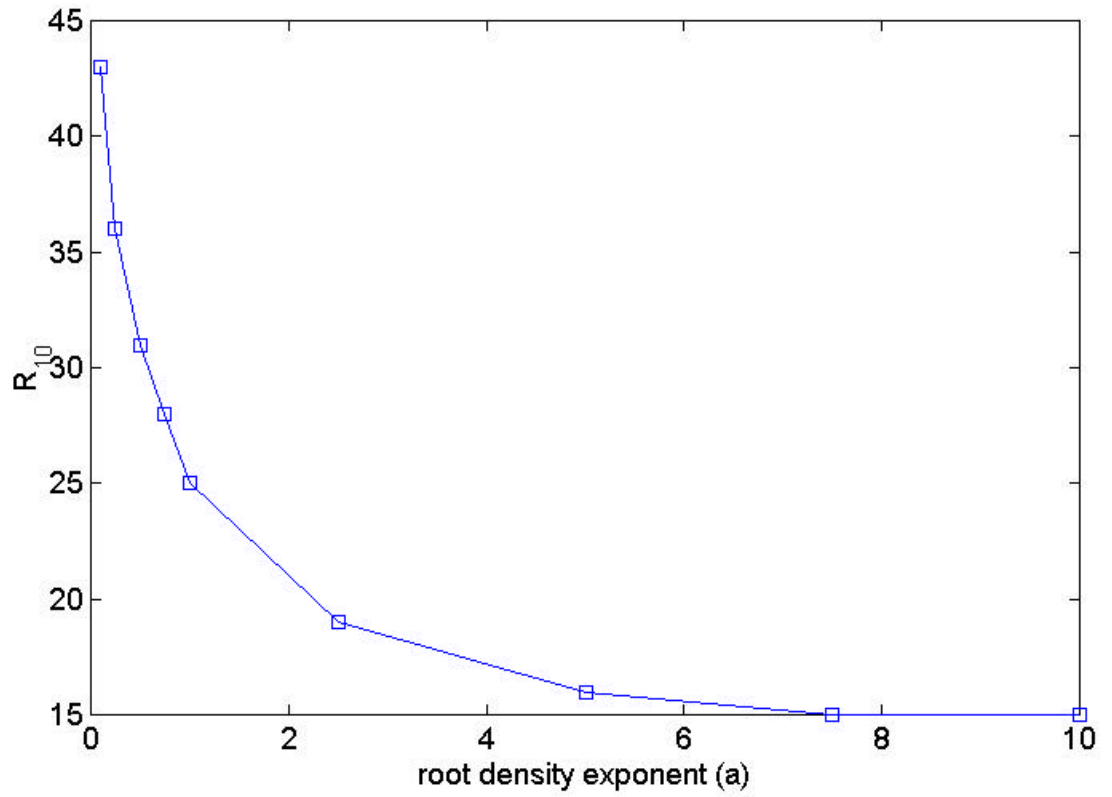


Figure 3.10 Percent of total roots within the top 10 cm of soil (R_{10}) for root density exponent values used for model simulations.

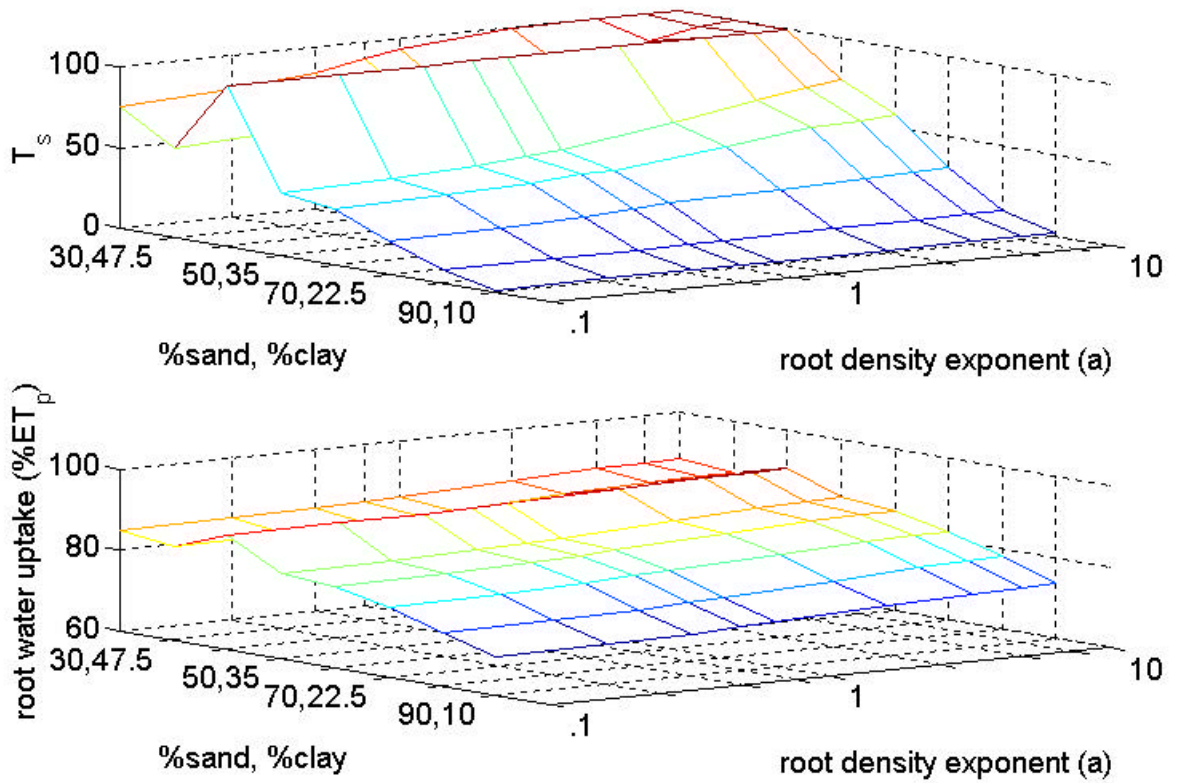


Figure 3.11 The percent of the model simulation time when the top 10 cm was $\geq 0.8\theta_s$ (T_s) and total root water uptake during model simulation for associated texture and root density distribution

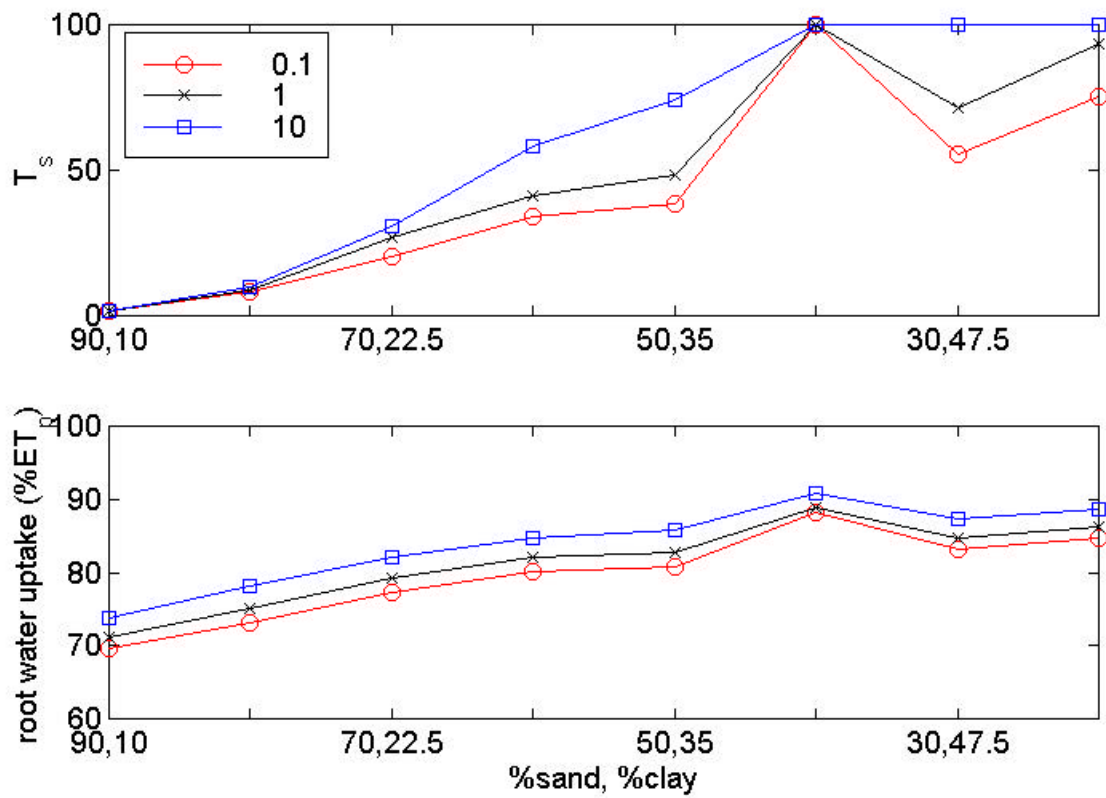


Figure 3.12 Values for T_s and total root water uptake for soil textures considered in the model simulations and root density exponents representative of grass, shrubs, and trees.

	%sand	%clay	θ_{sat}	K_{sat} (cm/min)	b	Ψ_{sat} (-cm)
sand	90	10	0.39	0.0523	6.5	12
loamy sand	80	16.3	0.43	0.0183	7.6	15
sandy loam	70	22.5	0.45	0.0084	8.3	22
sandy clay loam	60	28.8	0.48	0.0048	8.7	30
	50	35	0.49	0.0034	9	35
clay loam	40	41.3	0.51	0.0028	9.3	63
clay	30	47.5	0.52	0.0027	9.7	41
	20	53.8	0.54	0.0031	10.3	41

Table 3.1 Soil textures and associated soil hydraulic properties used in the modeling analysis of the effects of soil texture and root density distribution on saturation dynamics.

Chapter 4: General Conclusions and Implications

This thesis showed the relative importance of soil texture, elevation, and local root density in controlling tidal and vegetation control on soil moisture dynamics within a tidal marsh-forested upland transitional environment. The first part of the thesis examined the importance of both soil textural properties as well as elevation on the tidal control on soil moisture by both tidal inundation and tidally induced water table fluctuations. The second part determined numerically the joint role of soil texture and root density distribution with depth on the temporal distribution of soil saturation dynamics. Although vegetation type was shown to have an affect on soil saturation dynamics, it is also true that soil saturation dynamics will affect vegetation type. This feedback mechanism between vegetation controlling soil moisture and soil moisture controlling vegetation can be an important factor in the determination of the control of the dominant vegetation on temporal soil saturation dynamics for a specific ecosystem.

The analyses and results presented within this thesis have the general applicability to be used for land use planning purposes in coastal regions. On a global scale, the extent and health of salt marshes is on the decline (Zhang *et al*, 1997). Understanding the textural and elevation controls on the magnitude and extend of tidal fluctuations can be essential in predicting run-off generation in upland regions and the delivery of materials to vital marsh environments from activity such as land development and agricultural practices. The role that vegetation type has in controlling soil saturation dynamics determined by this study can further the understanding of saturation and run-off generation for upland regions with similar soil type and varying vegetation. Furthermore,

previous research has shown that even though salt marshes accumulate inorganic nutrients and heavy metals, daily tidal flushing will cause marsh sediments to release these materials back into tidal waters (reviewed in Harvey, 1986). Since tidal salt marsh environments can be considered low-lying buffer zones between forested upland areas and tidal waters, predicting saturated conditions that control the exchange surface water between upland regions and marsh environments also has significant implications for better understanding the magnitude of the flux of materials from marshes to tidal creeks.

Along with contributing to the prediction of run-off generation, this thesis can be important in contributing to the determination of vegetation dynamics and gas release from sediments along a marsh-upland transition. Brinson *et al* (1985) showed that the increased inundation and associated pore water salinity increased along marsh-upland gradients caused an increase in tree mortality, which led to the concept that the state change between upland and marsh is a function of tidally induced soil saturation (Brinson *et al*, 1995). The results from this study contribute to the overall understanding of the conditions that control the transformation from forested upland to tidal salt marsh environments through the determination of soil saturation as a function of tidally induced water table fluctuations beyond the extent of tidal inundation. Within tidal marsh environments, emissions of methane and sulfur gases are a function of anaerobic conditions associated with soil saturation and are important in prediction of radiation budgets (Bartlett *et al*, 1985; Nuttle and Hemond, 1988). The determination of soil saturation by tidal forcing as a function of soil texture and water table elevation presented in this study gives insight into the prediction of the spatial extent and frequency of occurrence of saturated conditions, which has implications for better predictions of

marsh-scale gas emissions given tidal and textural characteristics. Saturated conditions within forested upland environments mediate the release of gases such as nitrous oxide (Schapp *et al*, 1997). Prediction of soil saturation dynamics as a function of soil texture and vegetation type in upland fringe regions where the average water table elevation is low provides evidence of how vegetation type can control soil saturation within the same texture, thereby furthering the understanding of vegetation control on saturation, and associated gas release in this upland environment.

REFERENCES

- ASTM, 1981. Annual Book of ASTM Standards. American Society for Testing and Materials, Philadelphia, PA.
- Baird, J., Mason, T., and Horn, D., 1998. Validation of a Boussinesq model of beach ground water behavior. *Marine Geol.*, 148: 55-69.
- Bertness, M., 1985. Fiddler crab regulation of *Spartina alterniflora* production on a New England salt marsh. *Ecology*, 66: 1042-1055.
- Beven, K. and Kirkby, M., 1979. A physically based variable contributing area model of basin hydrology. *Hydrol. Sci. Bull.*, 24: 43-69.
- Bouten, W., Schaap, M., Bakker, D., and Verstraten, J., 1992. Modelling soil water dynamics in a forested ecosystem. I: A site specific evaluation. *Hydrol. Process.* 6: 435-444..
- Bouten, W., and Witter, J., 1992. Modelling soil water dynamics in a forest ecosystem. II: Evaluation of spatial variation of soil profiles. *Hydrol. Process.*, 6: 445-454.
- Brinson, M., Christian, R., and Blum, L., 1995. Multiple states in the sea-level induced transition from terrestrial forest to estuary. *Estuaries*, 18: 648-659.
- [Campbell Scientific, Inc. 1996. CS615 Water content reflectometer instruction manual, Logan, UT.](#)
- Christiansen, T, 1998. Sediment deposition on a tidal salt marsh. *Ph.D. dissertation*, Department of Environmental Sciences, University of Virginia.
- Clapp, R. and Hornberger, G., 1978. Empirical equations for some soil hydraulic properties. *Water Resour. Res.*, 14: 601-604.
- Feddes, R., 1971. Water, heat, and crop growth. *Thesis, Comm. Agr. Univ. Wageningen.*
- Feddes, R., Kowalik, P., Malinka, K., and Zaradny, H., 1976. Simulation of field water uptake by plants using a soil water dependent root water extraction function. *J. Hydrol.*, 31: 13-26.
- Feddes, R., Kowalik, P., and Zaradny, H., 1978. Simulation of field water use and crop yield. *Simulation Monograph*, Pudoc, Wageningen, The Netherlands, 9-30.
- Fetsko, M., 1990. A water balance estimate at Brownsville, Virginia. *Masters thesis*, Department of Environmental Sciences, University of Virginia.

- Gardner, L., Smith, B., Michener, W., 1992. Soil evolution along a forest-salt marsh transect under a regime of slowly rising sea level, southeastern United States. *Geoderma*, 55: 141-157.
- Harvey, J., 1986. Subsurface hydrology in a salt marsh *Masters thesis*, Department of Environmental Sciences, University of Virginia.
- Harvey, J., 1993. Measurement of variation in soil-solute tracer concentration across a range of effective pore sizes. *Water Resour. Res.*, 28: 1831-1837
- Harvey, J., Chambers, R., and Odum, W., 1988. Groundwater transport between hillslopes and tidal marshes. p. 270-276. In J. A. Kusler (ed.) Proceedings of the National Wetlands Symposium: Wetlands Hydrology. Association of State Wetland Managers, Berne, NY, USA.
- Harvey, J. and Odum, W., 1990. The influence of tidal marshes on upland groundwater discharge to estuaries. *Biogeochem.*, 10: 217-236
- Harvey, J. and Nuttle, W., 1995. Fluxes of water and solute in a coastal wetland sediment. 2. Effect of macropores on solute exchange with surface water. *J. Hydrol.*, 164: 109-125
- Harvey, J., Germann, P., and Odum, W., 1987. Geomorphological controls on subsurface hydrology in a creek bank zone of tidal marshes. *Estuarine Coastal Shelf Sci.*, 25: 677-691
- Hemond, H. and Fifield, J., 1982. Subsurface flow in salt marsh peat: a model and field Study. *Limnol. Oceanogr.*, 27: 126-136.
- Hemond, H.; Nuttle, W.; Burke, R.; Stolzenbach, K., 1984. Surface infiltration in salt marshes: Theory, measurement, and biogeochemical implications. *Water Resour. Res.*, 20: 591-600.
- Herkelrath, W., Miller, E., and Gardner, W., 1977. Water uptake by plants: II. The root contact model. *Soil Sci. Soc. Am. J.*, 41: 1039-1043.
- Hmieleski, J., 1994. High marsh-forest transitions in a brackish marsh: The effects of slope. *Masters thesis*, Department of Biology, East Carolina University.
- Hoogland, J., Feddes, R., and Belmans, C., 1981. Root water uptake model depending on soil water pressure head and maximum extraction rate. *Acta. Hort.*, 119: 123-136.
- Howes, B., Howrath R., Teal, J., and Valiela, I., 1981. Oxidation-reduction potentials in a salt marsh: spatial patterns and interactions with primary production *Limnol Oceanogr.*, 26: 350-360.

- Hughes, C., Binning, P., and Willgoose, G., 1998. Characterization of the hydrology of an estuarine wetland. *J. Hydrol.*, 211: 34-49
- Jackson, R., Canadell, J., Ehleringer, J., Mooney, A., Sala, O., and Schulze, E., 1996. A global analysis of root distributions of terrestrial biomes. *Oecologia*, 108: 389-411.
- Kastler, J., 1993. Sedimentation and landscape evolution of Virginia salt marshes. *Masters thesis*, Department of Environmental Sciences, University of Virginia.
- Kastler, J. and Wiberg, P., 1996. Sedimentation and boundary changes of Virginia salt marshes. *Estuarine Coastal Shelf Sci.*, 42: 683-700.
- Katul, G., Todd, P., Pataki, D., Kabala, Z., and Oren, R., 1997. Soil water depletion by oak trees and the influence of root water uptake on the moisture content spatial statistics. *Water Resour. Res.*, 33: 611-623.
- Knott, J.; Nuttle, W.; Hemond, H., 1987. Hydrologic parameters of salt marsh peat. *Hydrol. Process.*, 1: 211-220.
- Lai, C.-T., and Katul, G., 2000. The dynamic role of root-water uptake in coupling potential to actual transpiration. *Adv. Water Resour.*, 23: 427-439.
- Lanyon, J., Eliot, I., and Clarke, D., 1982. Groundwater level variation during semi-diurnal spring tide cycles on sandy beaches. *Aust. J. Mar. Freshwater Res.*, 33: 377-400.
- Li, L., Barry, D., Stagnitti, F., Parlange, J.-Y., and Jeng, D.-S., 2000a. Beach water table fluctuations due to spring-neap tide: moving boundary effects. *Adv. Water Resour.*, 23: 817-824.
- Li, L., Barry, D., Cunningham, C., Stagnitti, F., and Parlange, J.-Y., 2000b. A two-dimensional analytical solution of groundwater responses to tidal loading in an estuary and ocean. *Adv Water Resour.*, 23: 825-833.
- Li, L., Barry, D., Stagnitti, F., and Parlange, J.-Y., 2000c. Groundwater waves in a coastal aquifer: a new governing equation including vertical effects and capillarity. *Water Resour. Res.*, 36: 411-420.
- Li, L., Barry, D., and Pattiarachi, C., 1997. Numerical modeling of tide-induced beach water table fluctuations. *Coastal Eng.*, 30: 105-123.
- Mendelsohn, I. and Seneca, E., 1980. The influence of soil drainage on the growth of salt marsh cordgrass *Spartina alterniflora* in North Carolina. *Estuarine Coastal Marine Sci.*, 11: 27-40.

- Mixon, R., 1985. Stratigraphic and geomorphic framework of uppermost Cenozoic deposits in the southern Delmarva peninsula, Virginia and Maryland. *U.S.G.S. Professional Paper* 1067-G.
- Molz, F., 1981. Models of water transport in the soil-plant system: A review. *Water Resour. Res.*, 17: 1245-1260.
- Montaldo, N., and Albertson, J., 2001. On the use of the force-restore SVAT model formulation for stratified soils. *J. Hydrometeor.*, in press.
- Musters, P., and Bouten, W., 1999. Assessing rooting depths of an Austrian pine stand by inverse modeling soil water content maps. *Water Resour. Res.*, 35: 3041-3048.
- Musters, P., Bouten, W., and Verstraten, J., 2000. Potentials and limitations of modelling vertical distributions of root water uptake of an Austrian pine forest on a sandy soil. *Hydrol. Process.*, 14: 103-115.
- Nielsen, P., 1990. Tidal dynamics of the water table in beaches. *Water Resour. Res.*, 26: 2127-2134.
- Nuttle, W. and Harvey, J., 1995. Fluxes of water and solute in a coastal wetland sediment. 1. The contribution of regional groundwater discharge. *J. Hydrol.*, 164: 89-107.
- Nuttle, W. and Hemond, H., 1988. Salt marsh hydrology: Implications for biogeochemical fluxes to the atmosphere and estuaries. *Global Biogeochem. Cycles*, 2: 91-114.
- Perrochet, P., 1987. Water uptake by plant roots- a simulation model, I. Conceptual model. *J. Hydrol.*, 95: 55-61.
- Prasad, R., 1988. A linear root water uptake model. *J. Hydrol.*, 99: 297-306.
- Price, J. and Woo, M., 1988. Studies of a sub-arctic coastal marsh. 1. Hydrology. *J. Hydrol.*, 103: 275-292.
- Priestly, C. and Taylor, R., 1972. On the assessment of surface heat flux and evaporation using large scale parameters. *Mon. Weather Rev.*, 100: 81-92.
- Remson, I., Hornberger, G., and Molz, F., 1971. Numerical Methods in Subsurface Hydrology., John Wiley and Sons.
- Ridd, P., 1996. Flow through animal burrows in mangrove creeks. *Estuarine Coastal Shelf Sci.*, 43: 617-625.

- Saxton, K., Rawls, W., Romberger, J., and Papendick, R., 1986. Estimating generalized soil-water characteristics from texture. *Soil Sci. Soc. Am. J.*, 50: 1031-1036.
- Schaap, M., Bouten, W., and Verstraten, J., 1997. Forest floor water content dynamics in a Douglas fir stand. *J. Hydrol.*, 201: 367-383.
- Tan, K., 1996. Soil sampling, preparation, and analysis. *Books in soils, plants and the environment series.*, 73-82.
- Tiktak, A., and Bouten, W., 1992. Modeling soil water dynamics in a forested ecosystem. III. Model description and evaluation of discretization. *Hydr. Process.*, 6: 455-462.
- Tobon Marin, C., Bouten, W., and Dekker, S., 2000. Forest floor water dynamics and root water uptake in four forest ecosystems in northwest Amazonia. *J. Hydrol.*, 237: 169-183.
- Turaski, S., 2001. Saturation dynamics and sediment transport within a tidal salt marsh. *Masters thesis*, Department of Environmental Sciences, University of Virginia.
- United States Department of Agriculture (USDA), 1989. Soil survey of Northampton County, Virginia. *Soil Conservation Service*, pp. 94.
- White, E., Prichett, W., and Robertson, W., 1971. Slash pine root biomass and nutrient concentrations. *Miscellaneous Report-Maine Agricultural Experiment Station*, Orono, ME.
- Zhang, M., Ustin, S., Rejmankova, E., and Sanderson, E., 1997. Monitoring Pacific Coast salt marshes using remote sensing. *Ecol. Application.*, 7: 1039-1053.

APPENDIX A: Calibration Curve for CS615 Water Content Reflectometer

Due to the high pore water salinity along the study transect, the standard calibration equations for the CS615 probes relating probe period output and volumetric water content could not be used. The calibration equation determined by Campbell Scientific, Inc. for the CS615 probes is for pore water salinity of approximately 5 ppt (electroconductivity of 3.0 dSm^{-1}) (Campbell Scientific, 1996). Average pore water salinity along the study transect ranged from 5 ppt to 35 ppt. The calibration curve derived for this study was valid for the range of pore water salinity at the study transect for the summer of 1999. For probe period output between 0.7 msec and 5 msec, there was a second order polynomial relationship between volumetric water content in the top 30 cm of soil ($\theta_{30\text{cm}}$) and the probe period output (p), where

$$q_{30\text{cm}} = -.025223(p)^2 + .20958(p) - .036476 \quad (\text{A.1})$$

For probe period output above 5 msec, volumetric water content was determined to remain close to saturation ($\theta_{30\text{cm}}=0.40$), with hypersalinity conditions in the tidal study environment causing increased probe period output for the same volumetric water content.